Exotic compact objects in Einstein-Scalar-Maxwell theories

Antonio De Felice^{a*} and Shinji Tsujikawa^{b†}

^a Center for Gravitational Physics and Quantum Information,

Yukawa Institute for Theoretical Physics, Kyoto University, 606-8502, Kyoto, Japan

^b Department of Physics, Waseda University, 3-4-1 Okubo, Shinjuku, Tokyo 169-8555, Japan

(Dated: November 19, 2025)

In k-essence theories within general relativity, where the matter Lagrangian depends on a real scalar field ϕ and its kinetic term X, static and spherically symmetric compact objects with a positive-definite energy density cannot exist without introducing ghosts. We show that this no-go theorem can be evaded when the k-essence Lagrangian is extended to include a dependence on the field strength F of a U(1) gauge field, taking the general form $\mathcal{L}(\phi,X,F)$. In Einstein-scalar-Maxwell theories with a scalar-vector coupling $\mu(\phi)F$, we demonstrate the existence of asymptotically flat, charged compact stars whose energy density and pressure vanish at the center. With an appropriate choice of the coupling function $\mu(\phi)$, we construct both electric and magnetic compact objects and derive their metric functions and scalar- and vector-field profiles analytically. We compute their masses and radii, showing that the compactness lies in the range $\mathcal{O}(0.01) < \mathcal{C} < \mathcal{O}(0.1)$. A linear perturbation analysis reveals that electric compact objects are free of strong coupling, ghost, and Laplacian instabilities at all radii for $\mu(\phi) > 0$, while magnetic compact objects suffer from strong coupling near the center.

I. INTRODUCTION

The advent of gravitational-wave astronomy [1, 2] and very long baseline interferometry [3, 4] has opened new windows for probing physics in strong-gravity regimes. Black holes (BHs) are extremely compact objects with an event horizon, predicted as vacuum solutions [5, 6] to the Einstein equations in general relativity (GR) [7]. Neutron stars (NSs) are also compact objects without an event horizon, whose geometries are determined by including a baryonic matter source in Einstein equations, typically modeled as a perfect fluid. In addition to the presence or absence of the horizon, NSs have regular centers, whereas BHs typically feature singularities at their centers. The properties of BHs and NSs can be constrained by observations of gravitational waves emitted from their binary systems.

Cosmological observations indicate that about 95 % of the energy density in the present Universe consists of dark energy and dark matter [8–12]. While dark energy drives cosmic acceleration on large scales, dark matter can gravitationally cluster to form the large-scale structure of the Universe [13, 14]. Possible candidates for dark matter include (pseudo)-scalar fields such as axions [15–20], as well as vector fields such as dark photons [21–25]. The usual horizonless compact objects are composed of baryonic matter, but there are also possibilities that scalar or vector fields give rise to self-gravitating exotic compact objects (ECOs) [26–28].

One of the well-known examples of such ECOs is a boson star composed of a complex scalar field with a potential [29, 30]. For a real canonical scalar field ϕ with the kinetic term $X = -(1/2)\partial_{\mu}\phi\partial^{\mu}\phi$ and potential $V(\phi)$,

which is given by the Lagrangian $\mathcal{L} = X - V(\phi)$, it is known that static and spherically symmetric (SSS) configurations with a positive-definite energy density do not exist within the framework of GR [31]. This property also holds for noncanonical scalar fields described by a k-essence Lagrangian $\mathcal{L}(\phi, X)$, as long as the ghost-free condition $\partial \mathcal{L}/\partial X > 0$ is satisfied [32]. This is why the real scalar field is extended to a complex scalar field to realize the SSS configuration of boson stars.

In the case of vector fields, Wheeler et al. [33, 34] originally attempted to construct particle-like solutions, known as "geons," by studying electromagnetism within the framework of GR. However, these geons were found to be unstable. By considering a complex Abelian vector field with a mass term, it is possible to form gravitational solitons, known as Proca stars [35, 36], within the framework of GR. Such a massive vector field can be associated with dark photons, i.e., one of the candidates for dark matter. It is also possible to extend Maxwell's theory with a real vector field to nonlinear electrodynamics, described by a Lagrangian of the form $\mathcal{L}(F)$ [37, 38], where F denotes the gauge-field field strength. By appropriately designing the functional form of $\mathcal{L}(F)$, one can construct SSS solutions that are regular at the center (r=0), including nonsingular BHs [39–43]. However, it has been shown that such solutions are unstable due to a Laplacian instability along the angular direction near r = 0 [44].

Given that real scalar and vector fields face difficulties in realizing SSS ECOs without instabilities, an important question is what occurs in theories containing both fields—particularly interactions between the scalar and vector fields. For example, one can consider Einstein-Scalar-Maxwell (ESM) theories described by the Lagrangian $M_{\rm Pl}^2 R/2 + X + \mu(\phi) F$, where $M_{\rm Pl}$ is the reduced Planck mass, R is the Ricci scalar, and $\mu(\phi)$ is the scalar-vector coupling that depends on the scalar field ϕ [45–47].

^{*} antonio.defelice@yukawa.kyoto-u.ac.jp

[†] tsujikawa@waseda.jp

For a dilatonic coupling of the form $\mu(\phi) = \mu_0 e^{-\lambda \phi}$, there exists an exact SSS BH solution endowed with scalar and electric (or magnetic) charges [48, 49], featuring curvature singularities at r=0. By considering alternative forms of $\mu(\phi)$, it may be possible to realize star-like configurations that are free of singularities at their centers (see Ref. [50] for a charged boson star composed of a complex scalar field coupled to a real vector field).

Indeed, in theories described by the Lagrangian $M_{\rm Pl}^2R/2 + \mathcal{L}(\phi,X,F)$, the possibility of realizing compact objects with regular centers was studied in Ref. [51]. By examining several classes of theories encompassed by the matter Lagrangian $\mathcal{L}(\phi,X,F)$, no nonsingular BHs free of ghost or Laplacian instabilities have been found. However, there exist particular theories that allow the existence of horizonless compact objects without such instabilities. This includes ESM theories with the matter Lagrangian $\mathcal{L} = X + \mu(\phi)F$ mentioned above. Under the condition $\mu(\phi) > 0$, ghosts are absent, and the propagation speeds are luminal in both the radial and angular directions (see Refs. [52–54] for the analysis of perturbations in more general scalar-vector-tensor theories).

Although the possibility of realizing compact objects in ESM theories was proposed in Ref. [51], the profiles of the energy density and pressure have not yet been elucidated. In particular, it remains unclear how the no-go theorem for k-essence can be circumvented by incorporating the F dependence coupled to the scalar field. In this paper, we address this issue by computing the energy density, as well as the radial and transverse pressures, as functions of the radial coordinate r. To this end, we consider the case in which the ratio N(r) between the two metric functions is known as a function of r. We then derive analytic solutions for the metric functions, as well as for the scalar and vector field profiles.

In such a scenario, the same profiles of energy density and pressure are realized for both electric and magnetic objects, under appropriate choices of $\mu(\phi)$. In the magnetic case, the form of $\mu(\phi)$ is inversely related to that in the electric case, so that its functional dependence on ϕ differs between the two cases. We show that the energy density, which is positive for all r > 0, attains its maximum at an intermediate radius, while it vanishes at both r=0 and spatial infinity. We also plot the mass-radius relation by defining the radius r_s at which the mass function reaches 99 % of the total ADM mass M. For a given length scale r_0 , where each compact object is characterized by its own value of r_0 appearing in the function N(r), we find that M increases with r_s and asymptotically approaches the maximum value M_{max} . The compactness of charged objects can exceed the order of 0.01. We also find a universal relation between the ADM mass and the stellar radius, since M/r_s is fixed by the parameters of the Lagrangian once the criterion for determining the radius r_s is specified, as mentioned above.

While the ECOs realized in our models are free of ghost and Laplacian instabilities in both the electric and magnetic cases, it remains unclear whether such stars suffer from the strong coupling problem. Since this issue was not addressed in Ref. [51], we investigate it by considering perturbations around the SSS background. For the electric compact object, the coupling $\mu(\phi)$ diverges as $r \to 0$, and hence the vector-field perturbation is weakly coupled. In contrast, for the magnetic object, $\mu(\phi)$ approaches 0 as $r \to 0$, so that the vector-field perturbation becomes strongly coupled. Since nonlinear perturbations are out of control in the latter case, the background profile for the magnetic object loses its validity near the center. Therefore, the electric compact object is only the case in which the strong coupling problem is absent at any distance r. Even though $\mu(\phi)$ diverges at r=0, the interaction term $\mu(\phi)F$ is proportional to r^2 , and hence no divergence appears in physical quantities. Thus, linearly stable electric ECOs free from the strong coupling problem exist in ESM theories.

This paper is organized as follows. In Sec. II, we derive the field equations on the SSS background for theories described by the Lagrangian $M_{\rm Pl}^2 R/2 + \mathcal{L}(\phi, X, F)$, and show how the no-go theorem for k-essence can be circumvented. In Sec. III, we study the configurations of electric compact objects realized in ESM theories, with particular attention to the profiles of the energy density, radial and angular pressures, and the mass-radius relation. In Sec. IV, we show that the same density profile and massradius relation as those obtained for the electric object can be realized for the magnetic object by choosing the coupling $\mu(\phi)$ to be inversely proportional to that in the electric case. In Sec. V, we address the issue of strong coupling and show that only the electric compact object is free from this problem. Sec. VI is devoted to the conclusions.

II. FIELD EQUATIONS ON THE SSS BACKGROUND

We aim to construct nonsingular horizonless SSS objects with regular centers and study their properties. For this purpose, we introduce a real scalar field ϕ with the kinetic term $X=-(1/2)\partial_{\mu}\phi\partial^{\mu}\phi$, and a U(1) gauge field A_{μ} characterized by the field strength $F=-(1/4)F_{\mu\nu}F^{\mu\nu}$, where $F_{\mu\nu}=\partial_{\mu}A_{\nu}-\partial_{\nu}A_{\mu}$. We assume that these scalar and vector fields are present in the dark sector of the Universe. The gravitational sector is described by GR, whose dynamics is governed by the Einstein-Hilbert Lagrangian $M_{\rm Pl}^2R/2$. The total action is given by

$$S = \int d^4x \sqrt{-g} \left[\frac{M_{\rm Pl}^2}{2} R + \mathcal{L}(\phi, X, F) \right] , \qquad (2.1)$$

where g denotes the determinant of the metric tensor $g_{\mu\nu}$, and \mathcal{L} represents a function of ϕ , X, and F. The covariant equations of motion obtained by varying Eq. (2.1) with respect to $g^{\mu\nu}$ take the form

$$M_{\rm Pl}^2 G^{\mu}{}_{\nu} = T^{\mu}{}_{\nu} \,,$$
 (2.2)

where G^{μ}_{ν} is the Einstein tensor and T^{μ}_{ν} denotes the energy-momentum tensor of matter, expressed as

$$T^{\mu}_{\ \nu} = \mathcal{L}\,\delta^{\mu}_{\ \nu} + \mathcal{L}_{.X}\partial^{\mu}\phi\partial_{\nu}\phi + \mathcal{L}_{.F}F^{\mu}_{\ \lambda}F_{\nu}^{\ \lambda}\,,\tag{2.3}$$

with $\mathcal{L}_{X} \equiv \partial \mathcal{L}/\partial X$ and $\mathcal{L}_{F} \equiv \partial \mathcal{L}/\partial F$.

We take a SSS background described by the line element

$$ds^{2} = -f(r)dt^{2} + h^{-1}(r)dr^{2} + r^{2}(d\theta^{2} + \sin^{2}\theta d\varphi^{2}), \quad (2.4)$$

where f and h depend on the radial distance r. For horizonless compact objects, both f(r) and h(r) remain positive for all values of r. On this background, we consider the scalar field ϕ to depend only on the radial coordinate r. The theory (2.1) is invariant under the gauge transformation $A_{\mu} \to A_{\mu} + \partial_{\mu} \chi$, which ensures that the vector field has no longitudinal mode. In this case, we can choose the following configuration for A_{μ} :

$$A_{\mu} dx^{\mu} = A_0(r) dt - q_M \cos \theta \, d\varphi \,, \tag{2.5}$$

where $A_0(r)$ is a function of the radial coordinate r, and q_M is a constant associated with the magnetic charge. For this configuration, the scalar quantities X and F can be written as

$$X = -\frac{1}{2}h\phi'^2$$
, $F = \frac{hA_0'^2}{2f} - \frac{q_M^2}{2r^4}$, (2.6)

where a prime denotes a derivative with respect to the radial coordinate r.

From the (00), (11), and (22) [=(33)] components of the gravitational equation (2.2), we obtain

$$\frac{M_{\rm Pl}^2(rh'+h-1)}{r^2} = -\rho\,, (2.7)$$

$$\frac{M_{\rm Pl}^2[rhf' + f(h-1)]}{r^2f} = P_r, \qquad (2.8)$$

$$\frac{M_{\rm Pl}^2[2rfhf''-rhf'^2+(rh'+2h)ff'+2f^2h']}{4rf^2}$$

$$=P_t, (2.9)$$

where

$$\rho \equiv -T^{0}{}_{0} = \frac{hA_{0}^{\prime 2}}{f} \mathcal{L}_{,F} - \mathcal{L}, \qquad (2.10)$$

$$P_r \equiv T^1_1 = \mathcal{L} + h\phi'^2 \mathcal{L}_{,X} - \frac{hA_0'^2}{f} \mathcal{L}_{,F}, \quad (2.11)$$

$$P_t \equiv T^2_2 = \mathcal{L} + \frac{q_M^2 \mathcal{L}_{,F}}{r^4} \,.$$
 (2.12)

Here, ρ denotes the energy density sourced by ϕ and A_{μ} , while P_r and P_t correspond to the radial and transverse pressures, respectively. In contrast to a perfect fluid, P_r and P_t are generally not equal.

We define the mass function $\mathcal{M}(r)$ as

$$\mathcal{M}(r) \equiv 4\pi M_{\rm Pl}^2 r \left[1 - h(r)\right] \,.$$
 (2.13)

From Eq. (2.7), we then obtain the differential equation

$$\mathcal{M}'(r) = 4\pi\rho(r) r^2, \qquad (2.14)$$

whose solution can be expressed in the integrated form $\mathcal{M}(r) = \int_0^r 4\pi \rho(\tilde{r}) \, \tilde{r}^2 \mathrm{d}\tilde{r}$. The Arnowitt-Deser-Misner (ADM) mass of the SSS object is defined by the limit

$$M = \lim_{r \to \infty} 4\pi M_{\rm Pl}^2 r \left[1 - h(r) \right] , \qquad (2.15)$$

where the compactness of the object implies that M is constant.

Using the continuity equation, $\nabla_{\mu}T^{\mu}{}_{\nu}=0$, we obtain the following relation between the energy density and the pressures:

$$P'_{r} + \frac{f'}{2f}(\rho + P_{r}) + \frac{2}{r}(P_{r} - P_{t}) = 0, \qquad (2.16)$$

which can also be derived by combining Eqs. (2.7)-(2.9). The difference between P_r and P_t provides a modification to the continuity equation of a perfect fluid, $P'_r + f'(\rho + P_r)/(2f) = 0$. Using Eqs. (2.10)-(2.12), Eq. (2.16) can be written as

$$P'_{r} + \left(\frac{f'}{2f} + \frac{2}{r}\right)h\phi'^{2}\mathcal{L}_{,X} - \frac{2}{r}\left(\frac{hA_{0}^{2}}{f} + \frac{q_{M}^{2}}{r^{4}}\right)\mathcal{L}_{,F} = 0.$$
(2.17)

In k-essence theories, which are characterized by the Lagrangian $\mathcal{L}(\phi, X)$ [55–57], the third term on the lefthand side of Eq. (2.17) vanishes due to the property $\mathcal{L}_{F} = 0$. The absence of ghosts requires the condition $\mathcal{L}_{X} > 0$. The gravitational force is attractive when f'/f > 0, so that $P'_r(r) < 0$ for $\mathcal{L}_{F} = 0$. By applying the boundary condition $P_r(r \to \infty) = 0$, we obtain $P_r(r) > 0$ under the condition $P'_r(r) < 0$. At r = 0, we impose the condition $\phi'(0) = 0$ to avoid the appearance of a cusplike structure that would violate the SSS configuration. It then follows that $\rho(r=0) = -P_r(r=0) < 0$. This means that the energy density of the scalar field is negative. Thus, in k-essence theories satisfying the no-ghost condition, there exist no SSS objects with a positive energy density at the center [32]. This no-go theorem can be circumvented by including the F dependence in the k-essence Lagrangian.

We introduce the function

$$N(r) = \frac{f(r)}{h(r)}, \qquad (2.18)$$

which is positive to ensure the positivity of -g. Combining Eq. (2.8) with Eq. (2.7), we find

$$\frac{N'}{N} = \frac{r\phi'^2 \mathcal{L}_{,X}}{M_{\rm Pl}^2} \,. \tag{2.19}$$

The X dependence in \mathcal{L} implies $N' \neq 0$, resulting in a difference between f(r) and h(r). If \mathcal{L} does not depend on X, we have N' = 0, so that N(r) = 1 by imposing the boundary condition $f(r) = h(r) \to 1$ as $r \to \infty$.

Varying the action (2.1) with respect to A_0 and ϕ , we obtain

$$A_0' = \frac{q_E \sqrt{N}}{r^2 \mathcal{L}_E}, \qquad (2.20)$$

$$\left(\sqrt{N}hr^2\phi'\mathcal{L}_{,X}\right)' + \sqrt{N}r^2\mathcal{L}_{,\phi} = 0, \quad (2.21)$$

where q_E is an integration constant corresponding to the electric charge, and $\mathcal{L}_{,\phi} \equiv \partial \mathcal{L}/\partial \phi$. For a purely magnetically charged object $(q_E=0)$, the electric field A_0' vanishes, as expected. Equations (2.7), (2.19), (2.20), and (2.21) govern the background dynamics of our system. We note that Eq. (2.9) can be obtained by differentiating Eq. (2.19) and using the other equations of motion.

The energy density can be expressed as $\rho = A'_0 q_E/(r^2 \sqrt{N}) - \mathcal{L}$. By taking the derivative of Eq. (2.7) with respect to r, using the relation $\mathcal{L}' = \mathcal{L}_{,\phi} \phi' + \mathcal{L}_{,X} X' + \mathcal{L}_{,F} F'$, and eliminating $\mathcal{L}_{,F}$, $\mathcal{L}_{,X}$, $\mathcal{L}_{,\phi}$ terms by using Eqs. (2.7), (2.19), and (2.21), we obtain

$$4q_E r^2 A_0'^2 - M_{\rm Pl}^2 r^2 N^{-3/2} [2N^2 (r^2 h'' - 2h + 2) + rN(2rhN'' + 3rh'N' + 2hN') - r^2 hN'^2] A_0' + 4Nq_E q_M^2 / r^2 = 0.$$
 (2.22)

For SSS objects without curvature singularities at their center, the metric functions near r=0 must take the forms

$$h(r) = 1 + \sum_{n=2}^{\infty} h_n r^n,$$
 (2.23)

$$N(r) = N_0 + \sum_{n=2}^{\infty} N_n r^n, \qquad (2.24)$$

where h_n , N_0 , and N_n are constants. Substituting Eqs. (2.23) and (2.24) into Eq. (2.22) and expanding around r=0, the leading-order term of A_0' is given by $A_0' = \sqrt{N_0}\sqrt{-(q_Eq_M)^2/(q_Er^2)}$. Hence, a consistent solution exists only if $q_Eq_M=0$ [51]. Therefore, we focus on either the purely electric object $(q_E \neq 0, q_M=0)$ or the purely magnetic object $(q_M \neq 0, q_E=0)$.

In this paper, we study the properties of ECOs in ESM theories, where the matter sector is described by the Lagrangian

$$\mathcal{L} = X + \mu(\phi)F, \qquad (2.25)$$

with μ being a function of ϕ . In this case, Eqs. (2.10), (2.11), and (2.12) reduce, respectively, to

$$\rho = \frac{1}{2}h\phi'^2 + \frac{\mu A_0'^2}{2N} + \frac{\mu q_M^2}{2r^4}, \qquad (2.26)$$

$$P_r = \frac{1}{2}h\phi'^2 - \frac{\mu A_0'^2}{2N} - \frac{\mu q_M^2}{2r^4}, \qquad (2.27)$$

$$P_t = -P_r. (2.28)$$

It should be noted that using the relation $P_t + P_r = 0$ in Eqs. (2.8) and (2.9) yields a constraint equation for

the metric functions. The solutions that we study in the following sections automatically satisfy this constraint.

Ref. [51] studied linear perturbations around the background (2.1) and derived the stability conditions against odd- and even-parity perturbations for theories described by the action (2.1). For both electric and magnetic objects, the absence of ghosts requires that

$$\mathcal{L}_{,X} > 0, \qquad \mathcal{L}_{,F} > 0. \tag{2.29}$$

Since $\mathcal{L}_{,X}=1$ in ESM theories, the first condition is trivially satisfied. The second condition reduces to

$$\mathcal{L}_{F} = \mu(\phi) > 0. \tag{2.30}$$

The Lagrangian (2.25) contains only linear dependence on X and F, so that $\mathcal{L}_{,XX}=0,\,\mathcal{L}_{,FF}=0,\,$ and $\mathcal{L}_{,XF}=0.$ In this case, the propagation speeds of odd- and even-parity perturbations along both radial and angular directions are equal to the speed of light for both electric and magnetic objects [51]. This implies the absence of Laplacian instabilities in ESM theories.

Under the condition (2.30), the energy density given in Eq. (2.10) is positive. We also note that the third term on the left-hand side of Eq. (2.17) is negative, whereas the second term is positive for f'/f > 0. This allows for a region in which $P'_r(r) > 0$, so that $P_r(r)$ can become negative under the boundary condition $P_r(r \to \infty) = 0$. As long as $P_r(r = 0)$ is negative and the boundary condition $\phi'(0) = 0$ is imposed, the energy density at the center, $\rho(r = 0) = -P_r(r = 0)$, is positive. Therefore, the nogo theorem in k-essence theories—which forbids the SSS configuration with a positive-definite energy density—can be circumvented in ESM theories by introducing the F-dependence in \mathcal{L} .

Using the property $P_t = -P_r$, one can express Eq. (2.16) in the form

$$\hat{P}'_r + \frac{f'}{2f} \left(\hat{\rho} + \hat{P}_r \right) = 0,$$
 (2.31)

where

$$\hat{P}_r \equiv P_r + \int^r \frac{4}{\tilde{r}} P_r(\tilde{r}) d\tilde{r}, \qquad (2.32)$$

$$\hat{\rho} \equiv \rho - \int^{r} \frac{4}{\tilde{r}} P_{r}(\tilde{r}) d\tilde{r}. \qquad (2.33)$$

Equation (2.31) is analogous to the balance equation for a perfect fluid, with an effective energy density $\hat{\rho}$ and an effective radial pressure \hat{P}_r . Provided that $\hat{P}'_r < 0$, the pressure gradient \hat{P}'_r can counterbalance the gravitational force f'/(2f) $(\hat{\rho}+\hat{P}_r)$. In the following sections, we explicitly show that this behavior indeed occurs in ESM theories.

III. PURELY ELECTRIC OBJECTS

In this section, we focus on the purely electric case, characterized by

$$q_E \neq 0, \qquad q_M = 0. \tag{3.1}$$

Setting $q_M = 0$ in Eq. (2.22), the nonvanishing solution for the electric field is given by

$$A'_{0} = M_{\rm Pl}^{2} [2N^{2}(r^{2}h'' - 2h + 2) + rN(2rhN'' + 3rh'N' + 2hN') - r^{2}hN'^{2}]/(4N^{3/2}q_{E}).$$
(3.2)

Using Eq. (2.20), the coupling μ can be written as

$$\mu = \frac{q_E \sqrt{N}}{r^2 A_0'} \,. \tag{3.3}$$

Then, the energy density associated with the electric field, $\rho_E = \mu A_0^{\prime 2}/(2N)$, is expressed as

$$\rho_E = \frac{q_E A_0'}{2r^2 \sqrt{N}} \,. \tag{3.4}$$

For the scalar-field derivative appearing in Eq. (2.19), one can choose the positive branch of ϕ' without loss of generality, yielding

$$\phi' = M_{\rm Pl} \sqrt{\frac{N'}{rN}} \,. \tag{3.5}$$

The energy density associated with the scalar field, $\rho_{\phi} = h\phi'^2/2$, is given by

$$\rho_{\phi} = \frac{M_{\rm Pl}^2 h N'}{2rN} \,. \tag{3.6}$$

The sum of Eqs. (3.4) and (3.6) gives the total energy density, $\rho = \rho_E + \rho_{\phi}$. Using Eq. (2.7), the electric field can be written as

$$A_0' = -\frac{M_{\rm Pl}^2[2(rh'+h-1)N + rhN']}{q_E\sqrt{N}}.$$
 (3.7)

Substituting Eq. (3.7) into Eq. (3.3), we find

$$\mu = -\frac{q_E^2 N}{M_{\rm Pl}^2 r^2 [2(rh' + h - 1)N + rhN']} \,. \tag{3.8}$$

Using Eqs. (3.2) and (3.7), we obtain a differential equation relating the two metric functions:

$$2(r^{2}h'' + 4rh' + 2h - 2)N^{2} - r^{2}hN'^{2} + 3r(rh' + 2h)NN' + 2r^{2}hNN'' = 0.$$
 (3.9)

The solution to Eq. (3.9), consistent with the regularity condition of h(r) in Eq. (2.23), is

$$h(r) = \frac{2\int_0^r \sqrt{N(r_1)} (\int_0^{r_1} \sqrt{N(r_2)} dr_2) dr_1}{r^2 N(r)}, \quad (3.10)$$

where two integration constants must vanish to ensure regularity at r=0. Since N(r)>0, the function h(r) remains positive for all r>0, implying the absence of a horizon. In other words, ESM theories do not admit BH solutions with regular centers.

For a given functional form of N(r), the function h(r) can be obtained by integrating Eq. (3.10). Then, from Eqs. (3.5), (3.7), and (3.8), one can determine ϕ' , A'_0 , and μ , as functions of r. We note that A'_0 and μ contain the electric charge q_E , so that each of them depends on q_E . However, the energy density of the electric field,

$$\rho_E = -\frac{M_{\rm Pl}^2 [2(rh' + h - 1)N + rhN']}{2r^2N} \,, \tag{3.11}$$

does not explicitly depend on q_E . The same property also holds for ρ_{ϕ} , ρ , P_r , and P_t . This implies that, for a given function N(r), the quantities associated with the energy density and pressures—such as the mass and radius of the object—are independent of the choice of q_E .

Under the expansion of N(r) near r=0 given in Eq. (2.24), the leading-order contribution to Eq. (3.5) is $\phi'(r) = M_{\rm Pl} \sqrt{2N_2/N_0} + \mathcal{O}(r)$, which is nonvanishing at r=0. To avoid the formation of a cusp at r=0, which would violate the assumption of spherical symmetry, we require $N_2=0$. An example of a model satisfying $N_2=0$ is [51]

$$N = \left(\frac{r^4 + \sqrt{N_0} \, r_0^4}{r^4 + r_0^4}\right)^2 = \left(\frac{x^4 + \sqrt{N_0}}{x^4 + 1}\right)^2 \,, \qquad (3.12)$$

where N_0 and r_0 are positive constants, and

$$x \equiv \frac{r}{r_0} \,. \tag{3.13}$$

In this case, we have $\phi'(r) = 2M_{\rm Pl}\sqrt{N_4/N_0}\,r + \mathcal{O}(r^2)$ near r=0, with $N_4=2\sqrt{N_0}(1-\sqrt{N_0})/r_0^4$, and hence $\phi'(0)=0$. Since N_4 must be positive for the existence of the leading-order solution to $\phi'(r)$ around r=0, N_0 should be in the range

$$0 < N_0 < 1. (3.14)$$

Note that N(r) approaches 1 as $r \to \infty$, so that $f(r) \to h(r)$ in this limit. For $N_0 = 1$, we have N(r) = 1 for any r, and hence h(r) = 1 from Eq. (3.10). This corresponds to the Minkowski spacetime, in which ϕ' and A'_0 vanish; see Eqs. (3.5) and (3.7). In the opposite limit $N_0 \to 0$, the leading-order term of the Ricci scalar near the center, $R = 8(1 - \sqrt{N_0})r^2/(\sqrt{N_0}r_0^4)$, diverges, indicating the presence of a spacetime singularity. Therefore, we focus on the range $0 < N_0 < 1$.

For the choice (3.12), we can integrate Eq. (3.5) to find

$$\phi = \phi_0 + M_{\rm Pl}\lambda F\left(\arcsin\left(\frac{x^2}{\sqrt{x^4 + 1}}\right), -\frac{\lambda^2}{2}\right), \quad (3.15)$$

where F is the elliptic integral of the first kind, and

$$\lambda \equiv \sqrt{\frac{2(1-\sqrt{N_0})}{\sqrt{N_0}}}, \qquad (3.16)$$

so that $\lambda > 0$. Here, ϕ_0 is an integration constant corresponding to the field value at r = 0. For a given value of

 λ , N_0 is fixed to be $N_0 = 4/(\lambda^2 + 2)^2$. Since $\phi'(r) > 0$, the scalar field increases monotonically and reaches its maximum value at spatial infinity:

$$\phi_{\infty} = \phi_0 + M_{\rm Pl}\lambda K(-\lambda^2/2), \qquad (3.17)$$

where K denotes the complete elliptic integral of the first kind. The scalar field is in the range $0 \le \phi - \phi_0 < M_{\rm Pl}\lambda K(-\lambda^2/2)$. The relation between ϕ and $x = r/r_0$ in Eq. (3.15) can be inverted to give

$$x = \sqrt{\operatorname{sc}\left[\frac{\phi - \phi_0}{\lambda M_{\text{Pl}}}, -\frac{\lambda^2}{2}\right]}, \qquad (3.18)$$

where sc denotes the Jacobi elliptic function. As we will see below, the relation (3.18) allows us to express μ explicitly as a function of ϕ , i.e., $\mu = \mu[x(\phi)]$.

One can perform one of the integrals in Eq. (3.10), as

$$\int_0^r \sqrt{N(r_1)} \, dr_1 = r_0 \left(x - \frac{1 - \sqrt{N_0}}{2\sqrt{2}} \Delta_1 \right) , \qquad (3.19)$$

where

$$\Delta_1 \equiv \arctan\left(\sqrt{2}x + 1\right) + \arctan\left(\sqrt{2}x - 1\right) + \arctan\left[\sqrt{2}x/(x^2 + 1)\right]. \tag{3.20}$$

After performing the second integral in Eq. (3.10), it follows that

$$h = \frac{(x^4 + 1)^2}{8x^2 (x^4 + \sqrt{N_0})^2} \left[4\sqrt{2}\Delta_1 (\sqrt{N_0} - 1)x + \Delta_1^2 (\sqrt{N_0} - 1)^2 + 8x^2 \right].$$
 (3.21)

As we see from Eqs. (3.12) and (3.21), both N and h depend only on x and N_0 . After normalizing ρ_{ϕ} and ρ_{E} as $\tilde{\rho}_{\phi} = \rho_{\phi} r_{0}^{2}/M_{\rm Pl}^{2}$ and $\tilde{\rho}_{E} = \rho_{E} r_{0}^{2}/M_{\rm Pl}^{2}$ in Eqs. (3.6) and (3.11), respectively, the same property holds for $\tilde{\rho}_{\phi}$ and $\tilde{\rho}_{E}$. Therefore, the normalized energy density $\tilde{\rho} = \rho r_{0}^{2}/M_{\rm Pl}^{2}$ and the normalized pressures $\tilde{P}_{r} = P_{r} r_{0}^{2}/M_{\rm Pl}^{2}$ and $\tilde{P}_{t} = P_{t} r_{0}^{2}/M_{\rm Pl}^{2}$ do not explicitly depend on either r_{0} or q_{E} . This implies that the SSS configuration can be realized independently of the values of r_{0} and q_{E} , as we will confirm in the following.

By substituting Eqs. (3.12), (3.21), and their r derivatives into Eqs. (3.5), (3.7), and (3.8), we can analytically obtain $\phi'(r)$, $A_0'(r)$, and μ as explicit functions of r. It should be noted that both A_0' and μ depend on the electric charge q_E . Introducing the rescaled dimensionless charge,

$$\tilde{q}_E \equiv \frac{q_E}{M_{\rm Pl}r_0} \,, \tag{3.22}$$

one can express μ as

$$\mu = \tilde{q}_E^2 \mathcal{F}(x, N_0), \qquad (3.23)$$

where

$$\mathcal{F}(x, N_0) = -\frac{N}{x^2 [2\{xh'(x) + h - 1\}N + xhN'(x)]}.$$
(3.24)

Here, a prime denotes differentiation with respect to x. For given values of \tilde{q}_E and N_0 , we know μ as a function of $x = x(\phi)$. In other words, we have

$$\mu(\phi, \tilde{q}_E^2, \lambda) = \tilde{q}_E^2 \mathcal{F}[x = x(\phi, \lambda), N_0 = N_0(\lambda)]. \quad (3.25)$$

The function (3.25) is defined in the interval

$$0 \le \phi - \phi_0 < M_{\text{Pl}} \lambda K(-\lambda^2/2)$$
. (3.26)

Since the maximum field value is given by $\phi_{\infty} = \phi_0 + M_{\rm Pl}\lambda K(-\lambda^2/2)$, it is determined once ϕ_0 and λ are specified.

For a fixed value of \tilde{q}_E set by the theory, the corresponding electric charge q_E is determined by the free parameter r_0 . In the above relation, ϕ denotes a field, whereas λ and \tilde{q}_E are universal constants. Once the theory is specified, the values of λ and \tilde{q}_E are determined. This determines certain properties of the compact object under study, such as the value of N at its center. However, this does not single out a unique configuration for such compact objects, since r_0 remains a free parameter that must be specified. Only after fixing r_0 can one determine the ADM mass of the object, its charge, and all other physical properties. From a phenomenological point of view, once observations determine one of these quantities, say the ADM mass, all other physical properties of the object should then be uniquely determined. For instance, as already mentioned, $q_E/r_0 = \tilde{q}_E M_{\rm Pl}$, which is a universal constant.

A. Small-distance behavior

Let us examine the behavior of solutions around the center of electrically charged objects for the choice (3.12). Using Eq. (3.21) with the function (3.12), the metric functions near r = 0 can be expanded as

$$h = 1 - \frac{4\lambda^2}{5}x^4 + \mathcal{O}(x^8),$$
 (3.27)

$$f = N_0 \left[1 + \frac{\lambda^2}{5} x^4 + \mathcal{O}(x^8) \right].$$
 (3.28)

Therefore, h is a decreasing function of $x = r/r_0$ around the center, while f increases with x. Using Eqs. (3.5), (3.7), and (3.8), we also find the following properties near r = 0:

$$\frac{\mathrm{d}\phi}{\mathrm{d}x} = 2M_{\mathrm{Pl}}\lambda x + \mathcal{O}(x^5), \qquad (3.29)$$

$$\frac{dA_0}{dx} = \frac{8M_{\rm Pl}\lambda^2}{\tilde{q}_E(\lambda^2 + 2)}x^4 + \mathcal{O}(x^8), \qquad (3.30)$$

$$\mu = \frac{\tilde{q}_E^2}{4\lambda^2 x^6} + \mathcal{O}(x^{-2}). \tag{3.31}$$

One can integrate Eq. (3.29) to give

$$\phi = \phi_0 + M_{\rm Pl} \lambda x^2 + \mathcal{O}(x^6) \,. \tag{3.32}$$

Although μ diverges at r=0, the product μF in the Lagrangian (2.25) remains finite. In fact, since $F \propto r^8$, we have $\mu F \propto r^2$, which vanishes in the limit $r \to 0$. From Eqs. (3.31) and (3.32), the leading-order term of μ has the following ϕ dependence:

$$\mu(\phi) \simeq \frac{\tilde{q}_E^2 M_{\text{Pl}}^3 \lambda}{4(\phi - \phi_0)^3},$$
 (3.33)

which is positive. Therefore, the coupling must behave as $\mu(\phi) \propto (\phi - \phi_0)^{-3}$ to realize the form of N(r) in Eq. (3.12) near the center.

Expanding the energy density ρ and the pressures P_r and P_t around r = 0, it follows that

$$\rho = \frac{4M_{\rm Pl}^2 \lambda^2}{r_0^2} x^2 + \mathcal{O}(x^6) \,, \tag{3.34}$$

$$P_r = -P_t = -\frac{4M_{\rm Pl}^2 \lambda^4}{25r_0^2} x^6 + \mathcal{O}(x^{10}).$$
 (3.35)

In the limit $r \to 0$, all of ρ , P_r , and P_t vanish. This feature can be primarily attributed to the requirement $N_2 = 0$, introduced to ensure that $\phi'(r)$ vanishes at the origin. Unlike the usual case in which h(r) is expanded as $h(r) = 1 + h_2 r^2 + \cdots$ around r = 0, the next-to-leading order term of h(r) is proportional to r^4 .

Defining the equations of state as $w_r = P_r/\rho$ and $w_t = P_t/\rho$ for the radial and angular directions, respectively, their leading-order behavior near the center is given by

$$w_r = -w_t = -\frac{\lambda^2}{25} x^4 \,. \tag{3.36}$$

In the limit $x \to 0$, we have $|w_r| = w_t \ll 1$, indicating that the matter sector is in a nonrelativistic regime near the center. This behavior is markedly different from that in NSs [58] and gravastars with a de Sitter condensate core [59]. As r approaches r_0 , $|w_r|$ and w_t increase, potentially entering a relativistic regime characterized by $|w_r| = w_t \gtrsim \mathcal{O}(0.1)$. For smaller values of N_0 (i.e., larger λ), the magnitudes of $|w_r|$ and w_t near $r = r_0$ tend to be larger.

The effective radial pressure \hat{P}_r and energy density $\hat{\rho}$, defined in Eqs. (2.32) and (2.33), take the form

$$\hat{P}_r = C_0 - \frac{4M_{\rm Pl}^2 \lambda^4}{15r_0^2} x^6 + \mathcal{O}(x^{10}), \qquad (3.37)$$

$$\hat{\rho} = -C_0 + \frac{4M_{\rm Pl}^2 \lambda^2}{r_0^2} x^2 + \mathcal{O}(x^6) , \qquad (3.38)$$

where C_0 is an integration constant. Using Eqs. (3.28), (3.37), and (3.38), we find that the balance relation $d\hat{P}_r/dx = -8M_{\rm Pl}^2\lambda^4x^5/(5r_0^2) = -(\hat{\rho} + \hat{P}_r)(df/dx)/(2f)$, which corresponds to Eq. (2.31), is indeed satisfied.

B. Large-distance behavior

Let us proceed to study the behavior of solutions in the large-distance regime characterized by $r\gg r_0$. From Eqs. (3.12) and (3.21), the metric functions can be expanded as

$$h = 1 - \frac{\sqrt{2}\pi\lambda^2}{2(\lambda^2 + 2)x} + \frac{\pi^2\lambda^4}{8(\lambda^2 + 2)^2x^2} + \frac{8\lambda^2}{3(\lambda^2 + 2)x^4} + \mathcal{O}(x^{-5}), \qquad (3.39)$$

$$f = 1 - \frac{\sqrt{2}\pi\lambda^2}{2(\lambda^2 + 2)x} + \frac{\pi^2\lambda^4}{8(\lambda^2 + 2)^2x^2}$$

$$f = 1 - \frac{\sqrt{2\pi\lambda^2}}{2(\lambda^2 + 2)x} + \frac{\pi^2\lambda^4}{8(\lambda^2 + 2)^2x^2} + \frac{2\lambda^2}{3(\lambda^2 + 2)x^4} + \mathcal{O}(x^{-5}).$$
 (3.40)

The difference between h and f appears at order x^{-4} . Substituting Eq. (3.40) into the definition of the ADM mass M in Eq. (2.15), we find

$$M = \frac{2\sqrt{2}\pi^2\lambda^2}{\lambda^2 + 2}M_0, \qquad (3.41)$$

where

$$M_0 \equiv M_{\rm Pl}^2 r_0 = 2.7 \times 10^{-2} M_{\odot} \left(\frac{r_0}{1 \text{ km}}\right) ,$$
 (3.42)

and $M_{\odot} = 1.989 \times 10^{30}$ kg denotes the solar mass. In Sec. III D, we will study the mass-radius relation of the compact object in detail.

From Eqs. (3.5), (3.7), and (3.8), the large-distance behavior of $\mathrm{d}\phi/\mathrm{d}x$, $\mathrm{d}A_0/\mathrm{d}x$, and μ is given, respectively, by

$$\frac{\mathrm{d}\phi}{\mathrm{d}x} = \frac{2\sqrt{2}M_{\mathrm{Pl}}\lambda}{\sqrt{\lambda^2 + 2}} \frac{1}{x^3} + \mathcal{O}(x^{-7}), \qquad (3.43)$$

$$\frac{dA_0}{dx} = \frac{\pi^2 M_{\text{Pl}} \lambda^4}{4\tilde{q}_E (\lambda^2 + 2)^2} \frac{1}{x^2} + \mathcal{O}(x^{-4}), \qquad (3.44)$$

$$\mu = \frac{4\tilde{q}_E^2 (\lambda^2 + 2)^2}{\pi^2 \lambda^4} \left[1 - \frac{32(\lambda^2 + 2)}{\pi^2 \lambda^2} \frac{1}{x^2} + \mathcal{O}(x^{-3}) \right], \qquad (3.45)$$

where we have taken into account the next-to-leading order term in μ . One can integrate Eq. (3.43) to give

$$\phi = \phi_{\infty} - \frac{\sqrt{2}M_{\rm Pl}\lambda}{\sqrt{\lambda^2 + 2}} \frac{1}{x^2} + \mathcal{O}(x^{-6}).$$
 (3.46)

From Eqs. (3.45) and (3.46), the coupling $\mu(\phi)$ has the following dependence:

$$\mu(\phi) \simeq \frac{4\tilde{q}_E^2(\lambda^2 + 2)^2}{\pi^2 \lambda^4} \left[1 + \frac{16\sqrt{2}(\lambda^2 + 2)^{3/2}(\phi - \phi_\infty)}{\pi^2 M_{\text{Pl}} \lambda^3} \right].$$
(3.47)

As ϕ increases toward its asymptotic value ϕ_{∞} , the coupling $\mu(\phi)$ approaches the following constant:

$$\mu_{\infty} = \frac{4\tilde{q}_E^2(\lambda^2 + 2)^2}{\pi^2 \lambda^4} = \frac{4\tilde{q}_E^2}{\pi^2 (1 - \sqrt{N_0})^2}, \quad (3.48)$$

which is positive. In the region $r \ll r_0$, we recall that $\mu(\phi)$ decreases as a function of ϕ , i.e., $\mu(\phi) \propto (\phi - \phi_0)^{-3}$. To match this small-distance solution with the large-distance behavior given in Eq. (3.47), $\mu(\phi)$ must attain a minimum value μ_{\min} at an intermediate field value. To ensure the no-ghost condition $\mu(\phi) > 0$ for any value of ϕ , we require $\mu_{\min} > 0$. In Sec. III C, we will confirm that this condition is indeed satisfied.

Up to the order of r^{-2} , the metric functions h and f in Eqs. (3.39) and (3.40) can be written as $h=f=1-M/(4\pi M_{\rm Pl}^2 r)+q_E^2/(2M_{\rm Pl}^2\mu_\infty r^2)$. From Eq. (3.44), the electric field behaves as $A_0'(r)=q_E/(\mu_\infty r^2)$ at leading order, so that the SSS object has an effective electric charge q_E/μ_∞ . From Eq. (3.43), the derivative of the scalar field, $\phi'(r)$, decreases faster than r^{-2} at large distances. Therefore, the compact object does not possess a scalar charge.

We also find that, at large distances, the solutions for ρ , P_r , and P_t are given by

$$\rho = \frac{\pi^2 M_{\rm Pl}^2 \lambda^4}{8(\lambda^2 + 2)^2 r_0^2} \frac{1}{x^4} + \mathcal{O}(x^{-6}), \qquad (3.49)$$

$$P_r = -P_t = -\frac{\pi^2 M_{\rm Pl}^2 \lambda^4}{8(\lambda^2 + 2)^2 r_0^2} \frac{1}{x^4} + \mathcal{O}(x^{-7}), (3.50)$$

both of which are independent of q_E . The corresponding equations of state, $w_r = P_r/\rho$ and $w_t = P_t/\rho$, at leading order, are

$$w_r = -1, w_t = 1. (3.51)$$

Due to the property $w_r = -1$, the gravitational force $f'/(2f)(\hat{\rho} + \hat{P}_r)$ in Eq. (2.31), which is equivalent to $f'/(2f)(\rho + P_r)$, vanishes. Using the leading-order solution for P_r in Eq. (3.50), the effective pressure gradient \hat{P}'_r also vanishes, so that the balance relation (2.31) is satisfied at large distances.

C. Solutions covering the intermediate-distance regime

In Secs. III A and III B, we studied the properties of the solutions near r=0 and at large distances. In this section, we investigate the behavior of solutions at arbitrary distances r to understand how the two asymptotic solutions are connected in the intermediate region. Since we have an analytic solution for h(x) as well as for N(x), all other quantities, such as $\mathrm{d}\phi/\mathrm{d}x$, $\phi-\phi_0$, $\mathrm{d}A_0/\mathrm{d}x$, μ , ρ_ϕ , ρ_E , ρ , and $P_r=-P_t$, are determined for given values of N_0 and \tilde{q}_E . We also numerically integrate the differential equation (3.9) for h(x), starting from the vicinity of

x = 0. We confirm that the numerical solution for h(x) is in excellent agreement with the analytic one.

In Fig. 1, we plot f(x), h(x), and $\mathcal{M}(x)$ as functions of $x = r/r_0$ for $N_0 = 0.5$. These quantities are independent of the choice of \tilde{q}_E . Near the center, h(x) decreases from 1 as x increases. After reaching a minimum value $h \simeq 0.71$ at $x \simeq 1.45$, h(x) starts to increase toward its asymptotic value of 1. Since h(x) does not cross 0, the SSS object does not possess a horizon. Indeed, as shown in Eq. (3.10), this property holds for any value of N_0 in the range $0 < N_0 < 1$. As x increases, the mass function $\mathcal{M}(x)$ approaches a constant value, $M = 8.16 \, M_{\rm Pl}^2 r_0$, indicating that the object is compact. The other metric function, f(x), starts to vary from the value $N_0 = 0.5$ at the center and then continuously increases toward its asymptotic value of 1. Since the derivative f'(r) is always positive, the gravitational force is attractive, as expected.

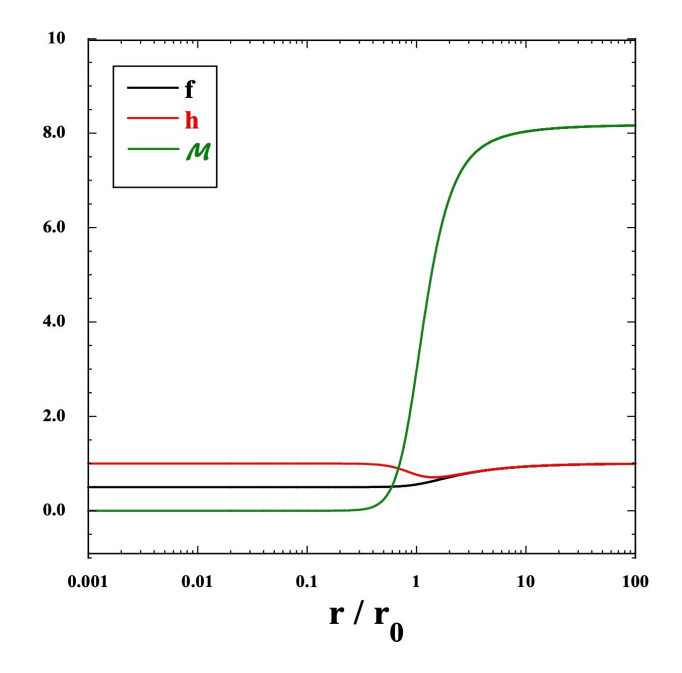


FIG. 1. Metric components f and h as functions of $x = r/r_0$ for $N_0 = 0.5$. We also show the mass function \mathcal{M} , which is normalized by $M_0 = M_{\rm Pl}^2 r_0$.

In Fig. 2, we show the profiles of $\tilde{q}_E A_0'$, ϕ' , and $\phi - \phi_0$ for $N_0 = 0.5$. As estimated from Eqs. (3.29) and (3.30), we find that $\phi'(r) \propto r$ and $A_0'(r) \propto r^4$ near r = 0. After reaching their maximum values, $\phi'(r)$ and $A_0'(r)$ start to decrease around $r = r_0$. In the region $r \gg r_0$, the field derivatives behave as $\phi'(r) \propto r^{-3}$ and $A_0'(r) \propto r^{-2}$, in agreement with the analytic estimates (3.43) and (3.44). Near r = 0, the scalar field increases as $\phi(r) - \phi_0 \propto r^2$. Asymptotically, $\phi(r)$ approaches its asymptotic value $\phi_\infty = \phi_0 + M_{\rm Pl}\lambda K(-\lambda^2/2)$.

In Fig. 3, we plot ρ , P_r , $\hat{\rho}$, and \hat{P}_r as functions of r/r_0 for $N_0=0.5$. For the computation of $\hat{\rho}$ and \hat{P}_r , we have set the integration constant \mathcal{C}_0 in the small-distance expansions of Eqs. (3.37) and (3.38) to 0. As in the case

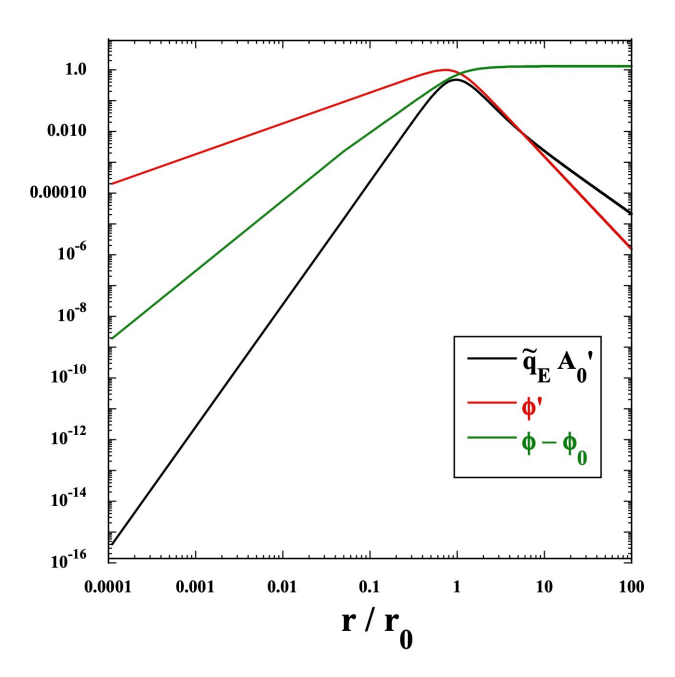


FIG. 2. Profiles of $\tilde{q}_E A_0'$, ϕ' , and $\phi - \phi_0$ as functions of $x = r/r_0$ for $N_0 = 0.5$. Each quantity is normalized by $M_{\rm Pl}/r_0$, $M_{\rm Pl}/r_0$, and $M_{\rm Pl}$, respectively.

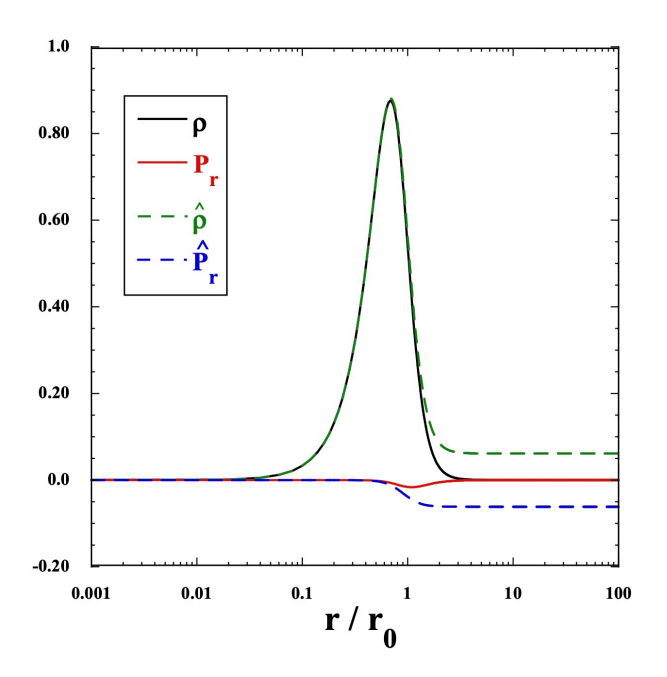


FIG. 3. Profiles of ρ , P_r , $\hat{\rho}$, and \hat{P}_r as functions of r/r_0 for $N_0=0.5$. All of these quantities are normalized by $M_{\rm Pl}^2/r_0^2$.

of the metric functions f and h, these quantities do not depend on the value of \tilde{q}_E . In Fig. 3, we observe that $\rho(r) > 0$ and $P_r(r) < 0$ at all radii r. Near the center (r=0), we have $\rho(r) \propto r^2$ and $-P_r(r) = P_t(r) \propto r^6$, as estimated from Eqs. (3.34) and (3.35), indicating that

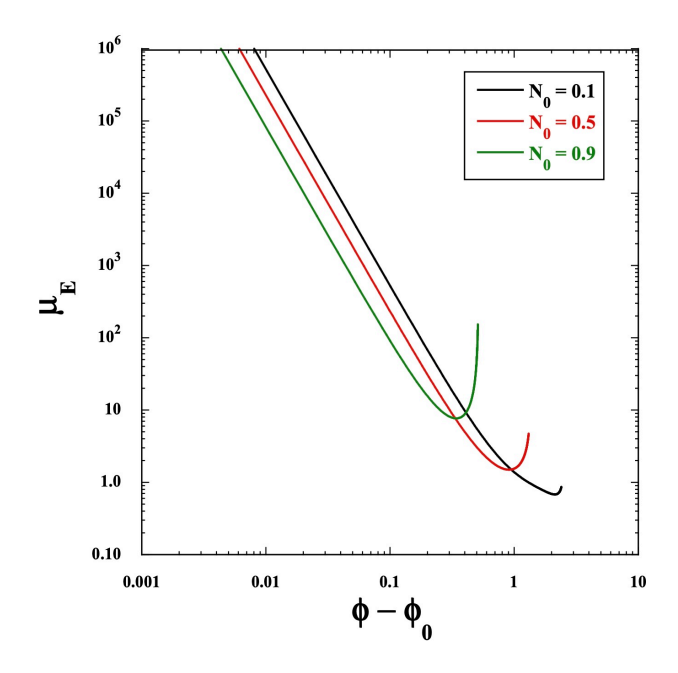


FIG. 4. The rescaled coupling $\mu_E = \tilde{q}_E^{-2}\mu$ as a function of $\phi - \phi_0$ (normalized by $M_{\rm Pl}$) with three different values of N_0 .

the matter fields are nonrelativistic with $|w_r| \ll 1$ and $w_t \ll 1$. After $\rho(r)$ and $|P_r(r)|$ reach their maximum values around $r = r_0$, they begin to decrease and exhibit the asymptotic behavior $\rho(r) \simeq -P_r(r) \propto r^{-4}$ in the region $r \gg r_0$. In Fig. 3, we observe that the effective radial pressure $\hat{P}_r(r)$, defined by Eq. (2.32), decreases monotonically, such that $\hat{P}'_r(r) < 0$. This negative effective pressure gradient counteracts the positive gravitational term, $f'/(2f)(\hat{\rho} + \hat{P}_r) = f'/(2f)(\rho + P_r) = f'/(2f)h\phi'^2$. At large distances, as seen in Fig. 3, we have $\hat{P}_r \simeq -\hat{\rho}$, and hence $P_r \simeq -\rho$ with $\hat{P}'_r(r) \simeq 0$. We also note that, for physical quantities such as P_r and ρ , we have $\lim_{r\to\infty} P_r = 0$ and $\lim_{r\to\infty} \rho = 0$, because we are considering asymptotically flat solutions. Thus, electric SSS compact objects with peculiar profiles of energy density and pressures exist in ESM theories. The key difference from stars composed of perfect fluids is that ρ , P_r , and P_t all vanish at r=0.

In Fig. 4, we plot the rescaled coupling

$$\mu_E \equiv \tilde{q}_E^{-2} \mu = \mathcal{F} \,, \tag{3.52}$$

as a function of $\phi - \phi_0$ for $N_0 = 0.1$, 0.5, and 0.9, where \mathcal{F} is defined in Eq. (3.24). We find that $\mu(\phi) \propto (\phi - \phi_0)^{-3}$ in the region where ϕ is close to ϕ_0 , that is, near r = 0. In the region $r \gg r_0$, the scalar field ϕ and the coupling μ asymptotically approach their respective values, $\phi_{\infty} = \phi_0 + M_{\rm Pl}\lambda K(-\lambda^2/2)$ and $\mu_{\infty} = 4\tilde{q}_E^2/[\pi^2(1-\sqrt{N_0})^2]$. As seen in Fig. 4, in the region where ϕ approaches ϕ_{∞} , the coupling $\mu(\phi)$ increases toward its asymptotic value μ_{∞} at $\phi = \phi_{\infty}$. This behavior is consistent with the analytic solution (3.47), which indicates that $\mu - \mu_{\infty}$ increases

linearly with ϕ . We also note that the numerical values of ϕ_{∞} and μ_{∞} in each case shown in Fig. 4 are in good agreement with the corresponding analytic estimates. In an intermediate regime of ϕ , the rescaled coupling $\mu_E(\phi)$ has a minimum value $\mu_{E,\min}$, which increases with N_0 . Since $\mu_{E,\min} > 0$ for values of N_0 in the range $0 < N_0 < 1$, the ghost-free condition $\mu(\phi) > 0$ is always satisfied.

D. Mass-radius relation

The ADM mass M of the electric object is analytically known from Eq. (3.41). In terms of N_0 , it can be expressed as

$$M = 2\sqrt{2}\pi^2 \left(1 - \sqrt{N_0}\right) M_0. \tag{3.53}$$

In the limit $N_0 \to 0$, the ADM mass reaches its maximum value

$$M_{\rm max} = 2\sqrt{2}\pi^2 M_0 = 0.75 M_{\odot} \left(\frac{r_0}{1~{\rm km}}\right)$$
 (3.54)

After normalizing the background equations of motion (2.7)-(2.9) with respect to $x=r/r_0$ and $\tilde{\rho}=\rho\,r_0^2/M_{\rm Pl}^2$, etc., they do not contain any explicit dependence on r_0 . Therefore, r_0 is an arbitrary positive constant. For $r_0=1$ km, the maximum mass is $M_{\rm max}=0.75M_{\odot}$. The ADM mass given in Eq. (3.53) vanishes in the limit $N_0\to 1$, which corresponds to the Minkowski spacetime where f(r)=h(r)=1 everywhere.

For a star composed of a perfect fluid, the standard definition of the radius r_s is the location where the radial pressure vanishes. In our case, the effective radial pressure P_r always decreases as a function of r, but it approaches a constant nonzero value at spatial infinity (see Fig. 3 for the choice $C_0 = 0$). Therefore, instead of using the pressure, we define the radius r_s as the point where the mass function $\mathcal{M}(r)$ reaches 99% of the ADM mass M, i.e., $\mathcal{M}(r_s) = 0.99 \, M$. This percentage can be chosen more flexibly, so we also consider the case in which the radius is determined by the condition $\mathcal{M}(r_s) = 0.90 M$. For given values of N_0 , the radius r_s can be computed using the analytic expression (3.21) for h, together with the definition (2.13) of the mass function. To verify the robustness of the results, we also numerically integrate Eq. (3.9) for h up to a sufficiently large distance, say $r = 10^6 r_0$, and compute the mass function to identify the radius according to the condition $\mathcal{M}(r_s) = 0.99 M$ (and also $\mathcal{M}(r_s) = 0.90 M$).

After obtaining M and r_s , we can compute the compactness of the object, which is defined by

$$C \equiv \frac{M}{8\pi M_{\rm Pl}^2 r_s} = \frac{1}{8\pi} \frac{M}{M_0} \frac{r_0}{r_s} \,. \tag{3.55}$$

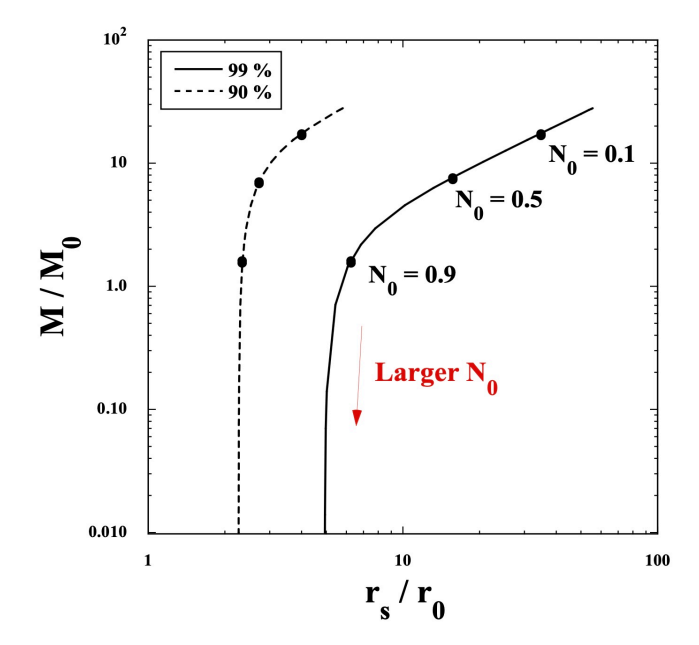


FIG. 5. The ADM mass M is plotted against the object's radius r_s , where M and r_s are normalized by $M_0 = M_{\rm Pl}^2 r_0$ and r_0 , respectively. The solid and dashed lines represent the cases where the radius is determined by the conditions $\mathcal{M}(r_s) = 0.99M$ and $\mathcal{M}(r_s) = 0.90M$, respectively. The black dots along both the solid and dashed lines correspond to the cases with $N_0 = 0.1$, 0.5, and 0.9.

The compactness increases with larger M or smaller r_s , but it is independent of r_0 . In other words, once a criterion for defining the radius is fixed, compactness becomes a universal property of these objects.

In Fig. 5, we show the mass-radius relation for values of N_0 in the range $0 < N_0 < 1$. The solid and dashed lines represent the cases where r_s is determined by the conditions $\mathcal{M}(r_s) = 0.99M$ and $\mathcal{M}(r_s) = 0.90M$, respectively. As N_0 increases from 0, both M and r_s decrease accordingly. To understand this behavior, we plot $\rho(r)$ as a function of r for $N_0 = 0.001, 0.1, 0.5, 0.9$ in Fig. 6. In the regime $r \ll r_0$, the energy density follows the behavior given by Eq. (3.34), such that $\rho(r)$ becomes smaller as N_0 increases toward 1. For larger N_0 , the maximum values of $\rho(r)$ reached at $r = r_m$ are also subject to decrease. Although r_m increases with larger N_0 , the radius r_s tends to decrease due to the shift of the $\rho(r)$ curves toward smaller r for $r > r_m$ (see Fig. 6). This explains the reduced values of r_s for increasing N_0 .

As N_0 decreases, the maximum energy density $\rho(r_m)$ increases, with r_m shifting toward smaller values. The product $\rho(r_m)r_m^2$ multiplied by r_s , i.e., $\mathcal{M}_0 \equiv \rho(r_m)r_m^2 r_s$, is roughly proportional to the ADM mass M of the object. As long as N_0 is not very close to 0, both $\rho(r_m)r_m^2$ and r_s increase as N_0 decreases (see Fig. 6), leading to increases in \mathcal{M}_0 and M. However, as N_0 approaches 0, the increases in $\rho(r_m)r_m^2$ and r_s become saturated, so that \mathcal{M}_0 , M, and r_s approach constant values. Therefore, for

¹ This implies that the radius corresponds to the value of $x_s = r_s/r_0$ at which $2x_s[1 - h(x_s)] - \sqrt{2}\pi(1 - \sqrt{N_0})\beta = 0$, where $\beta = 0.99$ is a chosen value.

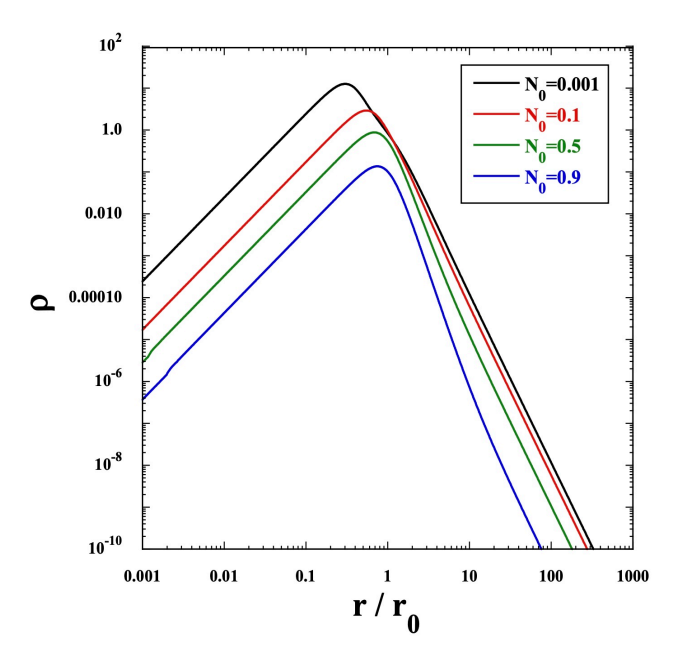


FIG. 6. The energy density ρ versus r/r_0 for four different values of N_0 , where ρ is normalized by $M_{\rm Pl}^2/r_0^2$.

a given r_0 , we obtain the maximum ADM mass given by Eq. (3.54). Using the condition $\mathcal{M}(r_s) = 0.99M$, the corresponding maximum radius is

$$(r_s)_{\text{max}} = 55.6 \, r_0 \,.$$
 (3.56)

For $r_0 = 2$ km, we have $(r_s)_{\rm max} = 1.12 \times 10^2$ km and $M_{\rm max} = 1.5 \, M_{\odot}$. The compactness corresponding to the maximum mass and the radius (3.56) is $\mathcal{C} = 0.02$. For $r_0 \gg 1$ km, it is possible to realize the SSS configuration with $M \gg M_{\odot}$ and $(r_s)_{\rm max} \gg \mathcal{O}(10 \text{ km})$.

As N_0 increases from 0 to 1, the ADM mass given by Eq. (3.53) decreases from M_{max} toward 0, while the radius r_s simultaneously becomes smaller than its maximum value given in Eq. (3.56). As an example, for $N_0 = 0.5$, we obtain $M = 8.18 M_0$ and $r_s = 16.7 r_0$, with a compactness of C = 0.02. This is much larger than the compactness of white dwarfs, $\mathcal{C} = \mathcal{O}(10^{-4})$. and that of the Sun, $C = \mathcal{O}(10^{-6})$, but still smaller than that of a BH, C = 1/2. For values of N_0 in the range $0 < N_0 \lesssim 0.7$, we find that M is approximately proportional to r_s , see Fig. 5. Therefore, the compactness remains nearly constant ($\mathcal{C} \simeq 0.02$). For $N_0 \gtrsim 0.9$, the ADM mass rapidly decreases below M_0 , resulting a compactness much smaller than $\mathcal{O}(10^{-2})$. In the limit $N_0 \to 1$, we have $N(r) \to 1$ at any distance r, and hence $h(r) \rightarrow 1$ from Eq. (3.21). In this limit, we also find $A_0'(r) \to 0$ and $\phi'(r) \to 0$ from Eqs. (3.2) and (3.5), so that the energy density $\rho(r) = h\phi'^2/2 + \mu A_0'^2/(2N)$ and the ADM mass M both vanish. Conversely, for N_0 close to 0, the variation of N(r) becomes maximal, leading to the largest values of $A'_0(r)$, $\phi'(r)$, and M.

The above results for the radius and compactness have

been obtained under the condition $\mathcal{M}(r_s) = 0.99M$. If we relax this condition to $\mathcal{M}(r_s) = 0.90M$, we find that the radius corresponding to the maximum ADM mass is given by $(r_s)_{\text{max}} = 5.8r_0$. This value is smaller by one order of magnitude than that in Eq. (3.56), so that the compactness increases to $\mathcal{C} = 0.19$. For $N_0 = 0.7$, we obtain $r_s = 2.53r_0$ and $M = 4.56M_0$, giving a compactness of $\mathcal{C} = 0.07$. For $N_0 \gtrsim 0.7$, the compactness rapidly drops below the order of 10^{-2} . In summary, a compactness of order $\mathcal{C} \gtrsim 10^{-2}$ can be achieved for $0 < N_0 \lesssim 0.7$ by adopting the criterion $0.90M \leq \mathcal{M}(r_s) \leq 0.99M$ for determining the radius of the object.

IV. PURELY MAGNETIC OBJECTS

We now proceed to study the purely magnetic object, characterized by

$$q_M \neq 0, \qquad q_E = 0, \tag{4.1}$$

under which $A_0'(r) = 0$, as follows from Eq. (2.20). Using Eq. (2.19) with the branch $\phi'(r) > 0$, we obtain $\phi'(r)$ in the same form as in Eq. (3.5). The corresponding energy density of the scalar field, $\rho_{\phi} = h\phi'^2/2$, is given by

$$\rho_{\phi} = \frac{M_{\rm Pl}^2 h N'}{2rN} \,,\tag{4.2}$$

which has the same form as Eq. (3.6) derived for the electric case. Substituting the energy density $\rho = h\phi'^2/2 + \mu q_M^2/(2r^4)$ into the background Eq. (2.7), the coupling μ can be expressed as

$$\mu = -\frac{M_{\rm Pl}^2 r^2 [2(rh' + h - 1)N + rhN']}{q_M^2 N} \,. \tag{4.3}$$

We introduce the dimensionless magnetic charge

$$\tilde{q}_M \equiv \frac{q_M}{M_{\rm Pl} r_0} \,, \tag{4.4}$$

and define

$$\mu_M \equiv \tilde{q}_M^2 \mu = \mathcal{F}^{-1} \,, \tag{4.5}$$

where \mathcal{F} is the function given in Eq. (3.24). Compared with the coupling (3.52) in the electric case, the following relation holds:

$$\mu_E \mu_M = 1 \,, \tag{4.6}$$

which demonstrates the electric-magnetic duality. The energy density associated with the magnetic charge, $\rho_M = \mu q_M^2/(2r^4)$, is given by

$$\rho_M = -\frac{M_{\rm Pl}^2[2(rh'+h-1)N+rhN']}{2r^2N}, \qquad (4.7)$$

which is of the same form as Eq. (3.11) in the electric case.

From Eq. (2.21), the ϕ derivative of μ can be expressed in the form:

$$\mu_{\phi} = \frac{2r^2}{q_M^2 \sqrt{N}} \left(\sqrt{N} h r^2 \phi' \right)'. \tag{4.8}$$

We differentiate Eq. (4.3) with respect to r and use the relation $\mu' = \mu_{,\phi} \, \phi'$. Substituting Eq. (4.8) together with $\phi' = M_{\rm Pl} \sqrt{N'/(rN)}$ into the right-hand side of this relation, we obtain

$$2(r^{2}h'' + 4rh' + 2h - 2)N^{2} - r^{2}hN'^{2} + 3r(rh' + 2h)NN' + 2r^{2}hNN'' = 0.$$
 (4.9)

which is the same form as Eq. (3.9) derived for the electric case. For a given function N(r), the integrated solution for h(r) can be found in the form of Eq. (3.10). From Eqs. (4.2) and (4.7), together with Eqs. (2.26)-(2.28), the energy density $\rho = \rho_{\phi} + \rho_{M}$ and the pressures P_{r} and P_{t} can be expressed in terms of the metric functions N(r) and h(r), as well as their derivatives. Thus, for a given N(r), we obtain the same solutions to h(r), f(r), $\mathcal{M}(r)$, $\phi'(r)$, $\rho(r)$, $P_{r}(r)$, and $P_{t}(r)$ as those in the electric case.

For the choice of N(r) given in Eq. (3.12), the metric function h(r) is analytically obtained in the form of Eq. (3.21), together with the mass function $\mathcal{M}(r)$ given in Eq. (2.13). The solution to the scalar field is given by Eq. (3.15), where ϕ_0 is the field value at r=0. The field value ϕ_{∞} at spatial infinity is related to ϕ_0 according to the relation (3.17). For $N_0=0.5$, the behaviors of f, h, \mathcal{M} , ϕ' , $\phi-\phi_0$, ρ , P_r , $\hat{\rho}$, and \hat{P}_r are the same as those shown in Figs. 1, 2, and 3, but without the electric field $(A'_0(r)=0)$.

As we showed in Eq. (4.6), the coupling μ_M is the inverse of μ_E defined in Eq. (3.52). Around the center of the body, the coupling has the following dependence:

$$\mu_M(\phi) \simeq \frac{4(\phi - \phi_0)^3}{M_{\rm Pl}^3 \lambda} \,,$$
 (4.10)

at leading order. Since the scalar field behaves as Eq. (3.32) near r=0, Eq. (4.10) translates to the radial dependence $\mu_M=4\lambda^2x^6\propto r^6$. At large distances, the coupling has the following ϕ dependence:

$$\mu_M(\phi) \simeq \frac{\pi^2 \lambda^4}{4(\lambda^2 + 2)^2} \left[1 - \frac{16\sqrt{2}(\lambda^2 + 2)^{3/2}(\phi - \phi_\infty)}{\pi^2 M_{\rm Pl} \lambda^3} \right],$$
(4.11)

where $\phi - \phi_{\infty} \simeq -\sqrt{2}M_{\rm Pl}\lambda/(\sqrt{\lambda^2 + 2}x^2)$. Thus, μ_M decreases as a function of ϕ (or r) toward its asymptotic value

$$\mu_{M,\infty} = \frac{\pi^2 \lambda^4}{4(\lambda^2 + 2)^2} = \frac{\pi^2 (1 - \sqrt{N_0})^2}{4} \,. \tag{4.12}$$

In Fig. 7, we plot μ_M as a function of $\phi - \phi_0$ for $N_0 = 0.1, 0.5, 0.9$. The coupling $\mu_M(\phi)$ increases proportionally to $(\phi - \phi_0)^3$ in the regime $\phi - \phi_0 \ll M_{\rm Pl}$,

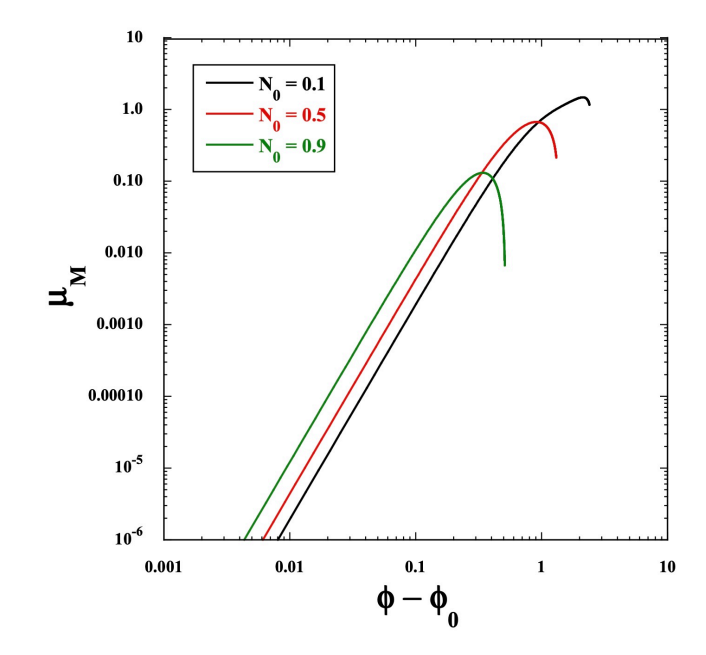


FIG. 7. The rescaled coupling $\mu_M = \tilde{q}_M^2 \mu$ as a function of $\phi - \phi_0$ (normalized by $M_{\rm Pl}$) with three different values of N_0 .

and then reaches a maximum. It subsequently decreases toward its asymptotic value $\mu_{M,\infty}$. As estimated from Eq. (4.11), $\mu_{M,\infty}$ decreases with increasing N_0 . Comparing Fig. 7 with Fig. 4, the theoretical curve of $\mu_M(\phi)$ corresponds to the reciprocal of $\mu_E(\phi)$.

With the choice (3.12) for N(r), the energy density profile $\rho(r)$ for a given value of N_0 is identical to that shown in Fig. 6. The relation between the ADM mass M and the radius r_s is also the same as that of the electric configuration plotted in Fig. 5. The ADM mass is analytically given by Eq. (3.53) as a function of N_0 . Defining the radius r_s by the condition $\mathcal{M}(r_s) = 0.99M$, we obtain the mass-radius relation shown as the solid line in Fig. 5. Relaxing the condition to $\mathcal{M}(r_s) = 0.90M$ shifts the (M, r_s) relation to the dashed line, yielding smaller radii r_s and larger compactness \mathcal{C} .

V. PERTURBATIONS AND STRONG COUPLING ISSUE

In theories described by the action (2.1), the secondorder action of perturbations around the background (2.4) was already derived in Ref. [51]. In that work, the authors also obtained the conditions for the absence of ghosts and Laplacian instabilities by taking the smallscale limit. In ESM theories where the matter sector is characterized by the Lagrangian $\mathcal{L} = X + \mu(\phi)F$, the theory is ghost-free for $\mu(\phi) > 0$. Indeed, as shown in Figs. 4 and 7, the coupling μ remains positive for both electric and magnetic configurations. Moreover, the propagation speeds of the five dynamical degrees of freedom coincide with the speed of light [51], ensuring the absence of Laplacian instabilities.

Thus, both the electric and magnetic compact objects realized in ESM theories are free from ghost and Laplacian instabilities. However, there remains one issue that was not addressed in Ref. [51]. For the compact objects studied in Secs. III and IV, the coupling $\mu(\phi)$ changes rapidly near r=0. In particular, when μ approaches 0 toward r=0, as in the case of the magnetic object, this may indicate the emergence of a strong coupling problem (see Ref. [60] for a similar situation arising in inflationary magnetogenesis). In the following, we address the issue of strong coupling.

We write the perturbations of the metric tensor $g_{\mu\nu}$ on the background (2.4), as $h_{\mu\nu}$, and then expand each component of them in terms of the spherical harmonics $Y_{lm}(\theta,\varphi)$ [61–64]. We consider the mode m=0 without loss of generality and write Y_{l0} as Y_l for simplicity. By choosing the gauge conditions $h_{t\theta}=0$, $h_{\theta\theta}=0$, $h_{\varphi\varphi}=0$, and $h_{\theta\varphi}=0$, the nonvanishing components of $h_{\mu\nu}$ are given by [65–68]

$$h_{tt} = f(r)H_{0}(t, r)Y_{l}(\theta), \quad h_{tr} = H_{1}(t, r)Y_{l}(\theta), h_{t\varphi} = -Q(t, r)(\sin\theta)Y_{l,\theta}(\theta), \quad h_{rr} = h^{-1}(r)H_{2}(t, r)Y_{l}(\theta), h_{r\theta} = h_{1}(t, r)Y_{l,\theta}(\theta), \quad h_{r\varphi} = -W(t, r)(\sin\theta)Y_{l,\theta}(\theta),$$
(5.1)

where H_0 , H_1 , H_2 , h_1 , Q, and W depend on t and r. We also decompose the scalar and vector fields, as

$$\phi = \bar{\phi}(r) + \delta\phi(t, r)Y_l(\theta), \tag{5.2}$$

$$A_{\mu} = \bar{A}_{\mu}(r) + \delta A_{\mu} , \qquad (5.3)$$

where

$$\delta A_t = \delta A_0(t, r) Y_l(\theta), \qquad \delta A_r = \delta A_1(t, r) Y_l(\theta),$$

$$\delta A_\theta = 0, \qquad \delta A_\varphi = -r \widetilde{\delta A}(t, r) (\sin \theta) Y_{l,\theta}(\theta). \tag{5.4}$$

The existence of the U(1) gauge invariance allows us to set $\delta A_{\theta} = 0$. Moreover, we multiplied $\widetilde{\delta A}(t,r)$ by r so that δA_{φ} can be written as $A_{\mu} \mathrm{d} x^{\mu} \ni -\widetilde{\delta A}(t,r) Y_{l,\theta}(\theta)(r\sin\theta\,\mathrm{d}\varphi)$, where $r\sin\theta\,\mathrm{d}\varphi$ is the orthonormal basis covector. Compared with the notation δA used in Ref. [51], the variables are related by $\delta A = r\widetilde{\delta A}$. The normalization with respect to $\widetilde{\delta A}$ is necessary when studying whether the solutions are strongly coupled.

In the odd-parity sector, the gauge-invariant combination of the form $\chi = r\dot{W} - rQ' + 2Q - 2\mathcal{L}_{,F}A'_0r\delta A/M_{\rm Pl}^2$ was introduced in Ref. [51], where a dot represents the derivative with respect to t. Analogous to δA_{φ} , we can express $h_{t\varphi}$ as $h_{t\varphi} = -(Q/r)(r\sin\theta)Y_{l,\theta}(\theta)$. The normalized field $\tilde{\chi}$ suitable for studying the issue of strong coupling should contain the term Q/r. Therefore, we introduce $\tilde{\chi} = \chi/r$, that is

$$\tilde{\chi} = \dot{W} - Q' + \frac{2Q}{r} - \frac{2\mathcal{L}_{,F} r A_0' \widetilde{\delta A}}{M_{\rm Pl}^2}.$$
 (5.5)

We also have the normalized odd-parity perturbation $\widetilde{\delta A} = \delta A/r$ arising from the covector field.

In the even-parity sector, Ref. [51] introduced a gauge-invariant combination arising from the gravitational sector, given by $\psi = rH_2 - Lh_1$. Since no additional factor of r is required for the proper normalization of H_2 , we define the rescaled field $\tilde{\psi} = \psi/r$, namely,

$$\tilde{\psi} = H_2 - \frac{Lh_1}{r} \,. \tag{5.6}$$

For the vector-field perturbation, we introduce the gaugeinvariant combination

$$\tilde{V} = r \left[\delta A_0' - \dot{\delta A}_1 + \frac{A_0'}{2} (H_0 - H_2) + \frac{A_0' \mu_{,\phi}}{\mu} \delta \phi \right], (5.7)$$

which is related to the variable V introduced in Ref. [51] through the relation $\tilde{V}=rV$. Defining \tilde{V} in this way ensures that the vector-field perturbation remains regular at spatial infinity. There is also a scalar-field perturbation $\delta\phi$ as a dynamical propagating degree of freedom in the even-parity sector.

A. Electric objects

Let us first consider the case of electric objects. Expanding the action (2.1) up to quadratic order in perturbations with the Lagrangian (2.25), the reduced second-order action takes the form

$$S^{(2)} = \int dt dr \, r^2 \sqrt{\frac{f}{h}} \left[K_{ab} \dot{\mathcal{X}}_a \dot{\mathcal{X}}_b - M_{ab} \mathcal{X}_a \mathcal{X}_b + \tilde{K}_{ij} \dot{\mathcal{Y}}_i \dot{\mathcal{Y}}_j - \tilde{M}_{ij} \mathcal{Y}_i \mathcal{Y}_j - \tilde{B}_{ij} (\dot{\mathcal{Y}}_i \mathcal{Y}_i - \mathcal{Y}_i \dot{\mathcal{Y}}_i) \right] , (5.8)$$

where the indices $a, b \in 1, 2$ label the odd-parity modes $\mathcal{X}_a \in \{\tilde{\chi}, \widetilde{\delta A}\}$, and the indices $i, j \in \{1, 2, 3\}$ label the even-parity modes $\mathcal{Y}_i \in \{\tilde{\psi}, \delta\phi, \tilde{V}\}$. The matrices K, M, \tilde{K} , and \tilde{M} are real and symmetric, whereas the matrix \tilde{B} is real but antisymmetric. In the square bracket of Eq. (5.8), the summation is taken over all the components a, b and i, j. We also note that the background determinant, excluding the angular part which has already been integrated, $\sqrt{-g} = r^2 \sqrt{f/h}$, appears explicitly in Eq. (5.8). This prescription is important for correctly addressing the issue of strong coupling.

The matrix K, which is associated with the odd-parity perturbations, has only diagonal components. The corresponding kinetic part of the Lagrangian $\mathcal{L}_K = r^2 \sqrt{f/h} \left(K_{11}\dot{\chi}^2 + K_{22}\dot{\delta}\dot{A}^2\right)$ can be written as $\mathcal{L}_K = r^2 \sqrt{f/h} \left[K_{11}f\left(\dot{\chi}/\sqrt{f}\right)^2 + K_{22}f\left(\dot{\delta}\dot{A}/\sqrt{f}\right)^2\right]$. In this form, we are considering the partial derivative $(1/\sqrt{f})\partial/\partial t$, where $\sqrt{f}dt$ represents the orthonormal infinitesimal

² Using the coordinate $z = \cos \theta$, we have exactly $\sqrt{-g} = r^2 \sqrt{f/h}$.

timelike interval, since \sqrt{f} is the lapse function.³ Therefore, after multiplying K_{11} and K_{22} by f, we obtain

$$K_{11}f = \frac{LM_{\rm Pl}^2}{4N(L-2)}\,, (5.9)$$

$$K_{22}f = \frac{L\mu}{2} \,, \tag{5.10}$$

where L = l(l+1). The positivity of $K_{11}f$ characterizes the ghost-free condition for the gravitational perturbation $\tilde{\chi}$. Since $K_{11}f$ is always positive, there is no ghost. At r = 0, we have $K_{11}f = LM_{\rm Pl}^2/[4N_0(L-2)]$, while at spatial infinity $K_{11}f \to LM_{\rm Pl}^2/[4(L-2)]$. Since $K_{11}f$ does not approach 0 at any radius r, the perturbation $\tilde{\chi}$ is not strongly coupled.

The other component, $K_{22}f$, remains positive for $\mu >$ 0, ensuring that the vector-field perturbation δA is ghostfree. Near r=0, we have $\mu \propto r^{-6}$, and hence $K_{22}f$ also increases proportionally to r^{-6} . This behavior corresponds to a weak-coupling limit for the vector-field perturbation δA . This is expected, since for this solution $\mu(\phi) \to +\infty$, and $\mu(\phi)$ multiplies the kinetic term F. At spatial infinity, $K_{22}f$ approaches a positive constant. The odd-parity vector-field perturbation is weakly coupled near the center, with no regime where δA becomes strongly coupled.

To investigate the strong coupling issue for even-parity perturbations, we need to diagonalize the kinetic matrix K_{ij} . One of the simplest ways to achieve this is by performing a field redefinition, $\mathcal{Y}_i = T_{ij}\bar{\mathcal{Y}}_j$, where T is a lower unitriangular matrix. In particular, this transformation leads to $\tilde{\psi}=\mathcal{Y}_1=\bar{\mathcal{Y}}_1,$ and $\bar{K}_{33}=$ $(T^t \tilde{K}T)_{33} = \tilde{K}_{33}$. Such a transformation always exists because det(T) = 1. Upon performing this step and taking the $l \gg 1$ limit, we find that the three diagonal elements are given by

$$\bar{K}_{11}f = \frac{\det(\tilde{K})f}{\tilde{K}_{22}\tilde{K}_{33} - \tilde{K}_{23}^2} = \frac{M_{\rm Pl}^2h^2}{L^2},$$
 (5.11)

$$\bar{K}_{22}f = \frac{(\tilde{K}_{22}\tilde{K}_{33} - \tilde{K}_{23}^2)f}{\tilde{K}_{33}} = \frac{1}{2},$$
 (5.12)

$$\bar{K}_{33}f = \tilde{K}_{33}f = \frac{\mu}{2LN},$$
 (5.13)

which are all positive for $\mu > 0$. As in the case of $K_{22}f$ for odd-parity modes, we have $\bar{K}_{33}f \to \infty$ for $r \to 0$ due to the behavior $\mu \propto r^{-6}$. This shows that the vectorfield perturbation V in the even-parity sector is weakly coupled near r = 0. At spatial infinity, $\bar{K}_{33}f$ approaches

a nonvanishing constant. The strong coupling problem does not arise for V at any radius r. The other components, $\bar{K}_{11}f$ and $\bar{K}_{22}f$, characterize the kinetic behavior of the remaining two dynamical perturbations in the even-parity sector. Since both $\bar{K}_{11}f$ and $K_{22}f$ approach constant values in the limits $r \to 0$ and $r \to \infty$, there are no strong coupling issues for ψ and $\delta \phi$.

Since $\bar{K}_{22}f = 1/2$, the field $\bar{\mathcal{Y}}_2$ is already canonically normalized. For the remaining two fields, the positivity of the normalized kinetic terms allows one to perform the final field redefinitions. By introducing $\bar{\mathcal{Y}}_1 = 2^{-1/2}L\hat{\mathcal{Y}}_1/(M_{\rm Pl}h)$ and $\bar{\mathcal{Y}}_3 = \sqrt{LN\hat{\mathcal{Y}}_3}/\sqrt{\mu}$, we obtain the canonical kinetic terms for $\hat{\mathcal{Y}}_1$ and $\hat{\mathcal{Y}}_3$, respectively. The fact that $\mu \to +\infty$ at the origin implies that terms higher than second order in perturbations are infinitely suppressed, leading to a decoupling behavior of the vector-field perturbation \tilde{V} . We have thus shown that electric objects are free from strong coupling problems in both the odd- and even-parity sectors.

Magnetic objects

We now proceed to the case of magnetic objects. After removing the nondynamical perturbations, the reduced second-order action can be expressed in the form

$$S^{(2)} = \int dt dr \, r^2 \sqrt{\frac{f}{h}} \left[\mathcal{K}_{ab} \dot{\mathcal{Z}}_a \dot{\mathcal{Z}}_b - \mathcal{B}_{ab} (\dot{\mathcal{Z}}_a \mathcal{Z}_b - \mathcal{Z}_a \dot{\mathcal{Z}}_b) \right. \\ \left. - \mathcal{M}_{ab} \mathcal{Z}_a \mathcal{Z}_b + \tilde{\mathcal{K}}_{ij} \dot{\mathcal{W}}_i \dot{\mathcal{W}}_j - \tilde{\mathcal{M}}_{ij} \mathcal{W}_i \mathcal{W}_j \right. \\ \left. - \tilde{\mathcal{B}}_{ij} (\dot{\mathcal{W}}_i \mathcal{W}_j - \mathcal{W}_i \dot{\mathcal{W}}_j) \right], \tag{5.14}$$

where $\mathcal{Z}_a \in \{\tilde{\chi}, \tilde{V}\}$ and $\mathcal{W}_i \in \{\tilde{\psi}, \delta\phi, \delta A\}$. All matrices are real and symmetric, except for \mathcal{B} and $\hat{\mathcal{B}}$, which are antisymmetric. Note that \mathcal{Z}_a consists of the oddparity gravitational perturbation $\tilde{\chi}$ and the even-parity vector-field perturbation V, while W_i contains the oddparity vector-field perturbation δA in addition to the even-parity modes ψ and $\delta\phi$.

The 2×2 matrix K, associated with the kinetic terms of the fields \mathcal{Z}_a , has both diagonal and off-diagonal components. We can diagonalize K by using a lower unitriangular matrix. Taking the $l \gg 1$ limit, we find that two diagonal components are given by

$$\bar{\mathcal{K}}_{11}f = \frac{(\mathcal{K}_{11}\mathcal{K}_{22} - \mathcal{K}_{12}^2)f}{\mathcal{K}_{22}} = \frac{M_{\text{Pl}}^2}{4N}, \qquad (5.15)$$

$$\bar{\mathcal{K}}_{22}f = \mathcal{K}_{22}f = \frac{\mu}{2LN}. \qquad (5.16)$$

$$\bar{\mathcal{K}}_{22}f = \mathcal{K}_{22}f = \frac{\mu}{2LN} \,.$$
 (5.16)

We also perform a similar procedure for the 3×3 matrix \mathcal{K} , which is associated with the fields \mathcal{W}_i . In the limit $l \gg$

 $^{^3}$ This is analogous to the normalization usually performed for the kinetic Lagrangian $\mathcal{L}_K = \sqrt{-g} \, Q(\dot{\psi}/\mathcal{N})^2$ on an isotropic cosmological background. Here, ψ denotes a perturbed field, and $\sqrt{-g} = \mathcal{N}a^3$, where a is the scale factor and \mathcal{N} is the lapse function. The time-dependent function Q represents the normalized kinetic coefficient, for which the strong coupling regime corresponds to the limit $Q \to 0$.

1, we obtain the following three diagonal components:

$$\overline{\tilde{\mathcal{K}}}_{11}f = \frac{\det(\tilde{\mathcal{K}})f}{\tilde{\mathcal{K}}_{22}\tilde{\mathcal{K}}_{33} - \tilde{\mathcal{K}}_{23}^2} = \frac{M_{\text{Pl}}^2h^2}{L^2}, \qquad (5.17)$$

$$\overline{\tilde{\mathcal{K}}}_{22}f = \frac{(\tilde{\mathcal{K}}_{22}\tilde{\mathcal{K}}_{33} - \tilde{\mathcal{K}}_{23}^2)f}{\tilde{\mathcal{K}}_{33}} = \frac{1}{2}, \qquad (5.18)$$

$$\overline{\tilde{\mathcal{K}}}_{22}f = \frac{(\tilde{\mathcal{K}}_{22}\tilde{\mathcal{K}}_{33} - \tilde{\mathcal{K}}_{23}^2)f}{\tilde{\mathcal{K}}_{33}} = \frac{1}{2},$$
 (5.18)

$$\overline{\tilde{\mathcal{K}}}_{33}f = \tilde{\mathcal{K}}_{33}f = \frac{L\mu}{2}. \tag{5.19}$$

All of Eqs. (5.15)-(5.19) are positive for $\mu > 0$, so that no ghosts arise in these solutions. However, both Eqs. (5.16) and (5.19) are proportional to μ . For magnetic objects studied in Sec. IV, the coupling μ behaves as $\mu \propto r^6$ near the center. This leads to vanishing kinetic coefficients for \tilde{V} and δA at r=0, so that these solutions are strongly coupled around the origin.

In other words, upon canonical normalization of the kinetic terms for \tilde{V} and δA , terms higher than second order in the perturbative expansion of the Lagrangian acquire $\sqrt{\mu}$ -dependent contributions in their denominators. As a result, the nonlinear terms dominate over the linear contributions in the limit $\mu \to 0$. In this regime, the analysis based on linear perturbations loses its validity near r=0, signaling the breakdown of the effective field theory.

In summary, the magnetic compact object, which is realized through the coupling μ in Eq. (4.3), is prone to the strong coupling problem around the center. This problem originates from the divergent behavior of F, which behaves as $F=-q_M^2/(2r^4)$ at the center. In this case, the coupling μ must offset the growth of F so that the product μF remains finite at r=0. Since the coupling depends as $\mu(\phi) \propto (\phi - \phi_0)^3 \propto r^6$, the system inevitably enters a strong coupling regime.

For electric objects, however, the field strength F behaves near the center as $F \propto r^8$, so that the product μF remains finite even if μ diverges at r=0. In this case, the coupling behaves as $\mu(\phi) \propto (\phi - \phi_0)^{-3} \propto r^{-6}$, corresponding to a weakly coupled regime. Although the same energy density, pressure, mass, and radius can be realized for both electric and magnetic objects, the two models are physically distinct due to the different functional dependences of the coupling $\mu(\phi)$. We have shown that only the electric object remains free from the strong coupling problem.

CONCLUSIONS

We studied the existence of regular ECOs without central singularities in a class of scalar-vector-tensor theories. In k-essence theories within the framework of GR, the absence of ghosts forbids static SSS solutions with a positive-definite energy density. By introducing the dependence of the gauge-field strength F in the k-essence Lagrangian, we showed that regular ECOs with positivedefinite energy can be achieved without ghosts.

In particular, we focused on ESM theories described by the Lagrangian $M_{\rm Pl}^2/2 + X + \mu(\phi)F$. We introduced the background density ρ and the radial and angular pressures P_r and P_t , as defined in Eqs. (2.10)-(2.12), to investigate the density profiles and the balance between the pressure gradient and gravity. As seen from the continuity equation (2.17), as long as $\mathcal{L}_{F} = \mu(\phi) > 0$, the pressure gradient induced by the coupling between the scalar and vector fields can counteract gravity.

For the electric object, we showed that the metric function h(r) can be written in the integrated form (3.10), where N(r) = f(r)/h(r). Since h(r) > 0 everywhere, the solution does not correspond to a BH but to an ECO without horizons. For the choice (3.12), we were able to obtain an analytic solution for h(r), given in Eq. (3.21), so that the background metric components are explicitly known. Accordingly, the scalar-field derivative ϕ' , the electric field A'_0 , the coupling μ , and the quantities ρ , $P_r (= -P_t)$ are all determined analytically. We showed that ρ vanishes at the center, with the nonrelativistic equation of state $w_r = P_r/\rho \to 0$. The energy density reaches a maximum around the radius $r = r_0$ and then decreases toward 0 at spatial infinity. The peculiar feature of the vanishing energy density and pressures is attributed to the fact that the form of N(r) is constrained by the boundary condition $\phi'(0) = 0$.

The coupling μ for the electric ECO is given by Eq. (3.8). Near r=0, μ behaves as $\mu \propto (\phi-\phi_0)^{-3}$, while at large distances its behavior is described by Eq. (3.47), so that $\mu(\phi)$ approaches a constant value μ_{∞} . The coupling exhibits a minimum at an intermediate distance, with a positive value for any N_0 in the range $0 < N_0 < 1$. Therefore, the ghost-free condition $\mu(\phi) > 0$ is satisfied at all distances r.

We also found that the ADM mass of the electric object is given by $M = 2\sqrt{2}\pi^2(1-\sqrt{N_0})M_0$, where $M_0 = M_{\rm Pl}^2 r_0$. For a given r_0 , M has a maximum value $M_{\rm max} = 2\sqrt{2\pi^2 M_{\rm Pl}^2} r_0$ in the limit $N_0 \rightarrow 0$. We defined the radius r_s of the object as the point where the mass function reaches 99% of the ADM mass, i.e., $\mathcal{M}(r_s) = 0.99M$. In this case, the maximum radius reached in the limit $N_0 \to 0$ is $(r_s)_{\text{max}} = 55.6r_0$. Since r_0 can take any positive value, both $M_{\rm max}$ and $(r_s)_{\rm max}$ can be arbitrarily large, while the ratio $M_{\rm max}/(r_s)_{\rm max}$ is fixed. In Fig. 5, we plot the mass-radius relation as a solid line, showing that both M and r_s decrease with increasing N_0 . The compactness of the object is approximately 0.02 for $0 < N_0 \lesssim 0.7$. Using an alternative criterion, $\mathcal{M}(r_s) = 0.90M$, to define the radius, the compactness can reach the order of 0.1.

For the magnetic ECO, the metric functions satisfy the differential equation (4.9), whose integrated solution coincides with Eq. (3.21) in the electric case. Consequently, with the choice of N(r) given by Eq. (3.12), the resulting forms of h(r) and f(r) are the same as those obtained in the electric configuration. Indeed, the functional dependence of ϕ' , as well as that of ρ and P_r (= $-P_t$), is identical in both the electric and magnetic cases. The

difference appears only for the coupling $\mu(\phi)$, where the rescaled magnetic coupling $\mu_M = \tilde{q}_M^2 \mu$ is related to the rescaled electric coupling $\mu_E = \tilde{q}_E^{-2} \mu$, as $\mu_M = \mu_E^{-1}$. Near the center of the body, the coupling behaves as $\mu_M \propto (\phi - \phi_0)^3$, approaching 0 as $r \to 0$. At spatial infinity, μ_M approaches the constant value $\pi^2 (1 - \sqrt{N_0})^2 / 4$. As shown in Fig. 7, $\mu_M(\phi)$ reaches a maximum at an intermediate field value.

For both the electric and magnetic objects, neither ghost nor Laplacian instabilities arise at any radius r. In this paper, we addressed the issue of strong coupling by properly introducing normalized dynamical perturbations on the SSS background. We showed that the electric object is free from this problem and that the vector-field perturbations remain weakly coupled near the center. On the other hand, the magnetic object suffers from the strong coupling problem of vector-field perturbations, as $\mu(\phi)$ approaches 0 in the limit $r \to 0$. Thus, only the electric configuration can serve as a viable candidate for an ECO without theoretical pathologies.

If a binary system containing at least one electric ECO exists, it should be possible to probe its signatures

through gravitational wave observations. During the inspiral phase of a binary coalescence, the gravitational waveform is expected to be influenced by the presence of electric charges associated with dark photons. As in the case of a scalar charge [69–73], the observed phase of the gravitational waveform should allow one to place bounds on the magnitude of the dark electric charge. Moreover, the Love number of ECOs is expected to differ from that of NSs [74, 75] due to the peculiar behavior of the density profile near the center. It could be constrained by future observations of the tidal deformability in binary systems containing ECOs. It would also be interesting to investigate whether such a compact-object configuration can arise from the collapse of scalar- and vector-field energy densities. A detailed analysis of these intriguing issues is left for future work.

ACKNOWLEDGEMENTS

ST is supported by JSPS KAKENHI Grant Number 22K03642 and Waseda University Special Research Projects (Nos. 2025C-488 and 2025R-028).

- [1] B. P. Abbott et al. (LIGO Scientific, Virgo), Phys. Rev. Lett. 116, 061102 (2016), arXiv:1602.03837 [gr-qc].
- [2] B. P. Abbott et al. (LIGO Scientific, Virgo), Phys. Rev. Lett. 119, 161101 (2017), arXiv:1710.05832 [gr-qc].
- [3] S. Doeleman et al., Nature 455, 78 (2008), arXiv:0809.2442 [astro-ph].
- [4] K. Akiyama et al. (Event Horizon Telescope), Astrophys. J. Lett. 875, L6 (2019), arXiv:1906.11243 [astro-ph.GA].
- [5] K. Schwarzschild, Sitzungsber. Preuss. Akad. Wiss. Berlin (Math. Phys.) 1916, 189 (1916), arXiv:physics/9905030.
- [6] R. P. Kerr, Phys. Rev. Lett. 11, 237 (1963).
- [7] A. Einstein, Annalen Phys. 49, 769 (1916).
- [8] N. Aghanim et al. (Planck), Astron. Astrophys. 641, A6 (2020), [Erratum: Astron.Astrophys. 652, C4 (2021)], arXiv:1807.06209 [astro-ph.CO].
- [9] D. Scolnic et al., Astrophys. J. 938, 113 (2022), arXiv:2112.03863 [astro-ph.CO].
- [10] T. M. C. Abbott et al. (DES), Astrophys. J. Lett. 973, L14 (2024), arXiv:2401.02929 [astro-ph.CO].
- [11] A. G. Adame et al. (DESI), JCAP 02, 021 (2025), arXiv:2404.03002 [astro-ph.CO].
- [12] M. Abdul Karim et al. (DESI), Phys. Rev. D 112, 083515 (2025), arXiv:2503.14738 [astro-ph.CO].
- [13] P. J. E. Peebles, Astrophys. J. Lett. 263, L1 (1982).
- [14] P. J. E. Peebles, Astrophys. J. 284, 439 (1984).
- [15] R. D. Peccei and H. R. Quinn, Phys. Rev. Lett. 38, 1440 (1977).
- [16] S. Weinberg, Phys. Rev. Lett. 40, 223 (1978).
- [17] F. Wilczek, Phys. Rev. Lett. 40, 279 (1978).
- [18] J. E. Kim, Phys. Rev. Lett. 43, 103 (1979).
- [19] M. A. Shifman, A. I. Vainshtein, and V. I. Zakharov, Nucl. Phys. B 166, 493 (1980).

- [20] D. J. E. Marsh, Phys. Rept. 643, 1 (2016), arXiv:1510.07633 [astro-ph.CO].
- [21] B. Holdom, Phys. Lett. B 166, 196 (1986).
- [22] P. Fayet, Nucl. Phys. B **347**, 743 (1990).
- [23] N. Arkani-Hamed, D. P. Finkbeiner, T. R. Slatyer, and N. Weiner, *Phys. Rev. D* **79**, 015014 (2009), arXiv:0810.0713 [hep-ph].
- [24] M. Pospelov and A. Ritz, Phys. Lett. B 671, 391 (2009), arXiv:0810.1502 [hep-ph].
- [25] M. Fabbrichesi, E. Gabrielli, and G. Lanfranchi, arXiv:2005.01515 [hep-ph].
- [26] F. E. Schunck and E. W. Mielke, Class. Quant. Grav. 20, R301 (2003), arXiv:0801.0307 [astro-ph].
- [27] S. L. Liebling and C. Palenzuela, Living Rev. Rel. 26, 1 (2023), arXiv:1202.5809 [gr-qc].
- [28] V. Cardoso and P. Pani, Living Rev. Rel. 22, 4 (2019), arXiv:1904.05363 [gr-qc].
- [29] D. J. Kaup, Phys. Rev. 172, 1331 (1968).
- [30] R. Ruffini and S. Bonazzola, Phys. Rev. 187, 1767 (1969).
- [31] G. H. Derrick, J. Math. Phys. 5, 1252 (1964).
- [32] A. Diez-Tejedor and A. X. Gonzalez-Morales, Phys. Rev. D 88, 067302 (2013), arXiv:1306.4400 [gr-qc].
- [33] J. A. Wheeler, Phys. Rev. 97, 511 (1955).
- [34] E. A. Power and J. A. Wheeler, Rev. Mod. Phys. 29, 480 (1957).
- [35] R. Brito, V. Cardoso, C. A. R. Herdeiro, and E. Radu, Phys. Lett. B 752, 291 (2016), arXiv:1508.05395 [gr-qc].
- [36] C. Herdeiro, E. Radu, and H. Rúnarsson, *Class. Quant. Grav.* **33**, 154001 (2016), arXiv:1603.02687 [gr-qc].
- [37] W. Heisenberg and H. Euler, Z. Phys. 98, 714 (1936), arXiv:physics/0605038.
- [38] M. Born and L. Infeld, Proc. Roy. Soc. Lond. A 144, 425 (1934).

- [39] E. Ayon-Beato and A. Garcia, Phys. Rev. Lett. 80, 5056 (1998), arXiv:gr-qc/9911046.
- [40] E. Ayon-Beato and A. Garcia, Phys. Lett. B 464, 25 (1999), arXiv:hep-th/9911174.
- [41] E. Ayon-Beato and A. Garcia, Phys. Lett. B 493, 149 (2000), arXiv:gr-qc/0009077.
- [42] K. A. Bronnikov, Phys. Rev. D 63, 044005 (2001), arXiv:gr-qc/0006014.
- [43] I. Dymnikova, Class. Quant. Grav. 21, 4417 (2004), arXiv:gr-qc/0407072.
- [44] A. De Felice and S. Tsujikawa, *Phys. Rev. Lett.* **134**, 081401 (2025), arXiv:2410.00314 [gr-qc].
- [45] M. K. Gaillard and B. Zumino, Nucl. Phys. B 193, 221 (1981).
- [46] M. J. Duff, J. T. Liu, and J. Rahmfeld, Nucl. Phys. B 459, 125 (1996), arXiv:hep-th/9508094.
- [47] L. Andrianopoli, M. Bertolini, A. Ceresole, R. D'Auria, S. Ferrara, P. Fre, and T. Magri, J. Geom. Phys. 23, 111 (1997), arXiv:hep-th/9605032.
- [48] G. W. Gibbons and K.-i. Maeda, Nucl. Phys. B 298, 741 (1988).
- [49] D. Garfinkle, G. T. Horowitz, and A. Strominger, *Phys. Rev. D* 43, 3140 (1991), [Erratum: Phys.Rev.D 45, 3888 (1992)].
- [50] V. Cardoso, C. F. B. Macedo, K.-i. Maeda, and H. Okawa, Class. Quant. Grav. 39, 034001 (2022), arXiv:2112.05750 [gr-qc].
- [51] A. De Felice and S. Tsujikawa, Phys. Rev. D 111, 064051 (2025), arXiv:2412.04754 [gr-qc].
- [52] L. Heisenberg, R. Kase, and S. Tsujikawa, Phys. Rev. D 97, 124043 (2018), arXiv:1804.00535 [gr-qc].
- [53] R. Gannouji and Y. R. Baez, JHEP 02, 020 (2022), arXiv:2112.00109 [gr-qc].
- [54] R. Kase and S. Tsujikawa, Phys. Rev. D 107, 104045 (2023), arXiv:2301.10362 [gr-qc].
- [55] C. Armendariz-Picon, T. Damour, and V. F. Mukhanov, Phys. Lett. B 458, 209 (1999), arXiv:hep-th/9904075.
- [56] T. Chiba, T. Okabe, and M. Yamaguchi, Phys. Rev. D 62, 023511 (2000), arXiv:astro-ph/9912463.

- [57] C. Armendariz-Picon, V. F. Mukhanov, and P. J. Steinhardt, Phys. Rev. Lett. 85, 4438 (2000), arXiv:astro-ph/0004134.
- [58] G. F. Burgio, H. J. Schulze, I. Vidana, and J. B. Wei, Prog. Part. Nucl. Phys. 120, 103879 (2021), arXiv:2105.03747 [nucl-th].
- [59] P. O. Mazur and E. Mottola, Universe 9, 88 (2023), arXiv:gr-qc/0109035.
- [60] V. Demozzi, V. Mukhanov, and H. Rubinstein, JCAP 08, 025 (2009), arXiv:0907.1030 [astro-ph.CO].
- [61] T. Regge and J. A. Wheeler, Phys. Rev. 108, 1063 (1957).
- [62] F. J. Zerilli, Phys. Rev. Lett. 24, 737 (1970).
- [63] V. Moncrief, Phys. Rev. D 10, 1057 (1974).
- [64] F. J. Zerilli, Phys. Rev. D 9, 860 (1974).
- [65] A. De Felice, T. Suyama, and T. Tanaka, Phys. Rev. D 83, 104035 (2011), arXiv:1102.1521 [gr-qc].
- [66] T. Kobayashi, H. Motohashi, and T. Suyama, Phys. Rev. D 85, 084025 (2012), [Erratum: Phys.Rev.D 96, 109903 (2017)], arXiv:1202.4893 [gr-qc].
- [67] T. Kobayashi, H. Motohashi, and T. Suyama, Phys. Rev. D 89, 084042 (2014), arXiv:1402.6740 [gr-qc].
- [68] R. Kase and S. Tsujikawa, Phys. Rev. D 105, 024059 (2022), arXiv:2110.12728 [gr-qc].
- [69] J. Alsing, E. Berti, C. M. Will, and H. Zaglauer, Phys. Rev. D 85, 064041 (2012), arXiv:1112.4903 [gr-qc].
- [70] N. Yunes, P. Pani, and V. Cardoso, Phys. Rev. D 85, 102003 (2012), arXiv:1112.3351 [gr-qc].
- [71] E. Berti, K. Yagi, and N. Yunes, Gen. Rel. Grav. 50, 46 (2018), arXiv:1801.03208 [gr-qc].
- [72] Y. Higashino and S. Tsujikawa, Phys. Rev. D 107, 044003 (2023), arXiv:2209.13749 [gr-qc].
- [73] H. Takeda, S. Tsujikawa, and A. Nishizawa, Phys. Rev. D 109, 104072 (2024), arXiv:2311.09281 [gr-qc].
- [74] E. E. Flanagan and T. Hinderer, Phys. Rev. D 77, 021502 (2008), arXiv:0709.1915 [astro-ph].
- [75] T. Hinderer, Astrophys. J. 677, 1216 (2008), [Erratum: Astrophys.J. 697, 964 (2009)], arXiv:0711.2420 [astro-ph].